Responses to Reviewer 1:
First, Thank you for your comments. We agree with many of the points brought up in the comments and will work to incorporate suggestions of both the technical and major comments. Many of the suggestions were in regard to improving organization and conciseness of the manuscript. This requires rearranging sections and a significant number of edits to sentence structure for clarity. We will undertake these changes, but for brevity, we do not include every planned sentence level edit in our response to reviewer comments at this time.

Major Comments:

1. *There is no doubt that the RICE ice core contains important information on climate and glaciological history in the Ross Sea region. The RICE age scale is essential to decoding this information and in my assessment the authors have done a good job with the age scale and this part clearly merits publication following some revision and restructuring. On the critical side, the sections on glaciological history of the Roosevelt Island and on methane variability are in my assessment much less mature than the age scale work and need to be substantially strengthened or removed all together. The methane findings are described as preliminary in the abstract and Climate of the Past should in my opinion not be publishing work that the authors believe is preliminary.*

   We have reorganized the manuscript to focus on the chronology development and what the chronology may tell us about the glaciology of Roosevelt Island. The introduction has been re-written, we have reduced how many times we describe development of the chronology, and we have removed section 5.1 "New observations of centennial-scale variability in the Holocene methane cycle". More specifics are given in response to other comments below.

2. *A further criticism is that the paper is excessively long, contains a lot of repetition and is not well structured – this makes it very tedious going for the reader. At present the paper reads more like a thesis than a journal article. Serious effort needs to be made by the author team to cut out information that is redundant to the results and conclusions presented.*

   This comment is addressed more specifically in our response to the technical comments, below.

3. *P6L1—4: An example figure is needed showing the straticounter annual layer selection.*

   We would prefer not to take up additional space in the paper with this. The depth-age relationship based on annual layer counts is already compared to the gas-based age scale in figure 7. For more information about annual layer selection, we would rather refer to [Winstrup et al. (2018)] (https://www.clim-past-discuss.net/cp-2017-101/) which describes in detail the data sets used for annual layer selection, the straticounter routine used to interpret count annual layers, and description of the seasonal patterns observed in those data sets. [Winstrup et al. (2018)] was recently revised and resubmitted so hopefully it will be fully published shortly.

4. *Section 5.1: There is no doubt that the centennial-scale methane variability is an interesting and important observation. However, in my view it should be the subject of a stand-alone paper, in which one would like to see detailed comparison of the various records and labelling of the methane trends that have been attributed to anthropogenic activity. As it stands the two paragraphs do not give a thorough treatment but still take up substantial space. If it must be included then I would suggest to scale back the section, certainly not so much introductory material is needed (it's not until near the final lines of the section that the RICE results are even referred to).*

   The relevant material on centennial-scale methane variability has been removed.

5. *Section 5.2: The first paragraphs appear to describe a thickening of the firn column going in to the LGM (25.3 to 21.8 ka) and an increase in accumulation rate. I find it surprising that accumulation rate would increase through the LGM and this observation merits some discussion. I note that the accumulation rate declines during the ACR as one would expect under cooler conditions.*

   This comment refers to the sentence:

   "After 25.3 ka, accumulation starts to increase and by the first δ^{15}N-N_2 maximum (21.8 ka), accumulation had increased to ~17 cm ice equivalent per year"

   found on p 13, L27-28 and also in Fig. 8d.

   We agree that the early increase in accumulation is an interesting feature. It is the solution that the firn model interprets for periods of increasing δ^{15}N-N_2 values. The alternative explanation for rising δ^{15}N-N_2 is cooling during this time, which is not supported by δD data. The surprise expressed by the reviewer likely stems from the widely held assumption that accumulation is closely linked to site temperature – this is true in a broad sense [Frieler et al. (2015)], but does not apply to millennial-scale variations at (coastal) sites where synoptic systems deliver much of the snowfall [Fudge et al. (2016)].

To address this comment, we have added the following:

"This feature is not apparent in other ice cores from the Ross Sea region, but those records tend to be difficult to interpret because of chronological uncertainties, such as is the case for Taylor Dome, Baggenstos et al (2017), or because of unexplained jumps in δ^{15}N-N_2, such as is the case for Siple Dome, Severinghaus et al. (2009)."

6. *The reconstruction and discussion of RICE accumulation history depends strongly on the questionable assumption that dD is a faithful recorder of temperature across the deglaciation. The potential for non-thermal effects on the dD record is critical and should be made earlier on in the paper (currently it is not until P14L25—30).*

   How Delta-age is affected by uncertainties in past temperature history is included in our description of the Delta-age sensitivity experiment on page 11. This is the earliest section which describes in detail the firn models used to estimate Delta-age. Although non-thermal effects are not specifically mentioned, a wide range of temperature histories is included in the sensitivity analysis. To be more explicit, some text has been added to p11, l33:

   "The sensitivity tests include a wide range of temperature histories so as to account for the possibility that some variations in δD were caused by non-thermal effects such as variability in precipitation seasonality, moisture sources and pathways, and post-depositional vapor exchange."

Technical comments:

1. *Abstract line 4. Clim. Past should not be in the business of publishing 'preliminary observations'. See major comments on whether these should be presented at all.*

   See response to Major comment 1, above. This line has been removed.

2. *Intro first para: The main focus of the paper is timescale development and the introduction should direct the reader to that subject from the*

start. Marine ice sheet stability does not come up again in the paper so does not need to be described here. Remove the para and I'd suggest replace with some sentences on importance of timescale development.

Thank you for the specific suggestions on how to tighten the manuscript. We have decided to revise the content of the introduction to focus on discussion of difficulties of developing chronologies for ice cores. To accomplish this, we have removed text describing history of the Ross Sea and MISI from the introduction and shifted text from section 4 which summarizes our strategy for chronology development. This reduces the text in section 4 (preceding section 4.1) and eliminates some redundancy.

3. *Intro second para: Here two scenarios are put forward for glaciological history in the Ross Sea region. The later discussion should more clearly refer back to the scenario which is supported by the new results. Since this glaciological history is not the primary focus of the paper I would suggest to move the paragraph to the end of the introduction.*

   This paragraph will be edited and moved to section 2.

4. *P2L35: No need to pers. comm. a co-author.*

   Removed reference to "personal communication".

5. *P3L14: This is the sort of information that is most relevant to the main age scale development task at hand and which belongs in the intro.*

   See response to technical comment 2. The manuscript has been rearranged so that the introduction will focus on the chronology development.

6. *Section 2. Para 2 of the intro could be better fit into this section renamed something like "Roosevelt Island ice core and glaciological history".*

   See response to technical comment 2. The manuscript has be rearranged and the description of Roosevelt Island and discussion of the significance its glaciology has been moved to Section 2.

7. *P4L20: I don't see any points in the RICE methane curve (Fig 3a) sitting 30 ppb above the WAIS curve. The legend does not inform which methane measurements are discrete and which are the problematic CFA.*

   Problematic samples discussed on P4L20 are not highlighted in Fig 3, but can be seen in the figure. We will work to make these measurements clearer by adding the continuous CH_4 records (currently light gray in Fig. 3a) to the figure legend and by making the continuous CH_4 line darker.

8. *P6L20: I don't think pers. comm. of a co-author is needed, remove here and throughout.*

   References of "personal communication" to work performed by coauthors has been removed.

9. *P6L5-15: The method used for each section of the core is repeated in the abstract, in line P3L5-20 and later again in the results. That's far too much repetition and testing of the readers patience. Its essential to revise the structure to avoid this repetition.*

   We will work to eliminate needless repetitions, but because the chronology development is a main contribution of the manuscript we feel that it warrants some inclusion in the abstract, introduction, and conclusion. The reviewer notes that we have also provided an overview of the chronology here (P5L5-15).

   We have reduced the text in this section (section 4 "Strategy for developing the chronology"). See edits described in response to technical comment 2.

10. *P6L18: Also repeats earlier material in Intro.*

    See response to technical comment 9.

11. *P6L30: "35% to 75% of the relevant variable": please clarify what is meant here.*

    We have re-written this sentence to be clearer, as follows:

    Original text:

    "The method starts with a set of prior ACPs which all correspond to well defined variations in either methane or $\delta^{18}O_{atm}$ (Table 1). Age uncertainty of ACPs was estimated from the length of time between 25% and 75% of the observed change of relevant variable."

    Revised text:

    "Prior ACPs all correspond to well defined increases or decreases of either methane or $\delta^{18}O_{atm}$. The age uncertainty of an ACP is assumed to be related to the duration of the corresponding increase or decrease. For this analysis we assume that the uncertainty (2 standard deviations) for an ACP corresponds to the time elapsed between 25% and 75% of the change in either methane or $\delta^{18}O_{atm}$ (Table 1)."

12. *Fig 5d): Please explain to the reader why there is a large difference between the "best realization", judged in terms of the goodness of fit, and the number of occurrences of a particular fit.*

    Added text to be inserted before P8,L18:

    "The best age estimate (realization) is not necessarily the same as the most frequent age estimate. Fig. 5d shows an example from sample depth 621.28 m where there is a large difference between these two age estimates. Large differences can occur because the prior age estimate (i.e. the age estimate based only on prior ACPs) differs by a large amount from the "true" age of that sample and because the goodness-of-fit parameter considers the fit over the whole record. In the case of the sample at 621.28 m, most realizations resulted in an age estimate of this sample of 9200 yr BP, similar to its prior age estimate of 9,240 yr BP, but the best realization estimated the age to be 9012 yr BP. There are two possible reasons for this type of result: 1) that this realization is the best because it managed to push the age of this sample by >200 years towards younger ages while not significantly changing the ages of nearby sections which already fit well, or 2) that no significant improvement in the goodness-of-fit was found by adjusting the age of this depth, and the goodness-of-fit was dictated by other sections of the record."

13. *Section 4.1: it would help the reader if this section referred right at the start to Fig 5.*

    Figure 5 is now referred to at the beginning of section 4.1 to show prior ACPs (white triangles in Fig. 5a) and a comparison between RICE and WAIS Divide CH_4 and $\delta^{18}O_{atm}$ on the final age scale (Fig. 5a-b).

14. *P9L3: I think its now the 4th time I read this.*

    See response to Technical comment 9. We removed this line.

15. *P9l15—19: As someone who works with these records I find this very hard to follow. Please revise for clarity.*

    Original text (full paragraph quoted for context):

    "Buizert et al. (2015) found that the annual layer counted portion of the GICC05modelext chronology (0-60 ka) (Andersen et al., 2006; Svensson et al., 2008) is systematically younger than ages of corresponding features found in the U/Th absolute dated Hulu speleothem record. A fit to Hulu ages was optimized by scaling the GICC05modelext ages linearly by 1.0063. For the target records we adopt the same scaling as Buizert et al. (2015) for the annual layer counted section of NGRIP, ending at 60 ka in the GICC05modelext chronology and equating to 60.378 ka in WD2014 (and RICE17). Ages older than 60 ka in the GICC05modelext chronology are derived from the ss09sea Dansgaard-Johnsen model (Johnsen et al., 2001; NGRIP Community Members, 2004) which is not susceptible to under counting of annual layers. This portion of GICC05modelext was stitched to the annual layer counts by subtracting a constant 705 years (Wolff et al., 2010). For this section of the target NGRIP records, a constant 378 years is added to the age from GICC05modelext starting at the depth corresponding to 60 ka in the GICC05modelext (60.378 ka in WD2014)."

Revised text (edits in red):

"Buizert et al. (2015) found that the annual-layer-counted portion of the GICC05modelext chronology (0-60 ka) (Andersen et al., 2006; Svensson et al., 2008) is systematically younger than ages of corresponding features found in the U/Th absolute dated Hulu speleothem record. A fit to Hulu ages was optimized by scaling the GICC05modelext ages linearly by 1.0063. This suggests that on average 6.3 out of every 1000 annual layers were not counted. For our NGRIP-based target records, we adjust the NGRIP age scale by adopting the scaling of Buizert et al. (2015). Older ages in the GICC05modelext chronology are derived from the ss09sea Dansgaard-Johnsen model (Johnsen et al., 2001; NGRIP Community Members, 2004). To make this section continuous with the adjusted annual layer counted section, we have added a constant 378 years (0.0063*60,000) for depths older than 60 ka in the target GICC05modelext ages."

16. *Section 4.3: Shorten it.*

    We will edit this section to shorten it.

17. *P11L7: The delta-age is established using a firn densification model, in which the modelling relies on a RICE temperature history derived from dD. The temperature history is thus integral to the development of the age scale of the ice, however the dD-based temperature reconstruction is cited as a pers. comm. I think the authors need to refer to a published temperature history or include the temperature history here... returning from coffee break... ok reading further down I see there are some more details on the assumptions in the temperature reconstruction and comparison to borehole data. Remove the pers. comm and see major comments.*

Our estimates of Delta-age, which will me made available with the paper, are dependent on assumptions regarding the temperature history. This record will be made publicly available in a forthcoming community manuscript from the RICE project. As described in the paper we account for uncertainties in Delta-age which result from our assumptions with a Monte-Carlo approach. We include chronological uncertainties, uncertainties in the assumptions in deriving a temperature history, uncertainty in constraints due to measurement error, and uncertainties from non-temperature related effects within the δD record.

Reference to "personal communication" will be removed.

18. *P12L24: Good. Agreed.*

19. *Section 5.1: There is no doubt that this discussion of methane variability is interesting. In my view it should be the subject of a stand-alone paper, in which one would like to see detailed comparison of the various records and labelling of the methane trends that have been attributed to anthropogenic activity. As it stands the two paragraphs do not give a thorough treatment but still take up substantial space. If it must be included then I would suggest to scale back the section, certainly not so much introductory material is needed (it's not until near the final lines of the section that the RICE results are even referred to).*

    See response to major comment 4. This section will be removed.

20. *Fig 4d. Adjust the y limits so we can more easily see the age uncertainty.*

    The axes in Figure 4d have been adjusted.

21. *P13L33: Include the uncertainty in the onset of the d15N change at 14.71 ka; I'm far from convinced that it significantly precedes onset of Bølling at 14.64 ± .19 ka.*

    The age of the depletion in $\delta^{15}N\text{-}N_2$ unambiguously precedes the onset of the Bølling, which is defined by an abrupt increase in CH_4, because both events are recorded in gas-phase measurements and the change in $\delta^{15}N\text{-}N_2$ is observed at a deeper depth than the change in CH_4. We have edited the text from:

    "Curiously, this abrupt decrease in $\delta^{15}N\text{-}N_2$ precedes the increase in CH_4 marking the onset of the Bølling-Allerød."

    To:

"Curiously, this abrupt decrease in $\delta^{15}N-N_2$ is observed in samples deeper than the increase in CH_4 marking the onset of the Bølling-Allerød meaning that this climate event unambiguously precedes the Northern Hemisphere event."

I have attached a figure which shows the $\delta^{15}N-N_2$ and CH_4 records during the deglaciation plotted versus depth.

22. *P14L11: This interesting sentence suffers from being way too long.*

    See response to technical comment 22. We have shortened it.

23. *P14L19–40: It would be more logical and much easier for the reader to follow your arguments if you set out the preferred explanation first and then explain, briefly, why some potential alternative explanations are unlikely. I don't find the preferred explanation very convincing: I don't see any quantitative data to support it, only some arm waving analogy to recent periods.*

    Changes to P14 L5-30 were made in accordance with the reviewer's suggestion on how to organize the discussion of possible interpretations.

24. *Section 5.3: It would help the reader to refer early in the section to the "maximum" and "fast and thin" Denton (1989) scenarios that were set up in the introduction.*

    We will make this change.

25. *P15L4: Again refer to the scenario set up in the introduction, here and elsewhere in this section.*

    We will make this change.

26. *P15L18: Refer to the dD record in Fig3b. Not to a pers comm!*

    Reference to "personal communication" will be removed.

    We would like to note that δD is not shown in Fig 3b. What is shown it the $^{18}O/^{16}O$ ratio for O2.

27. *P15L26: The comment about an MBL ice dome comes out of the blue and its far from obvious who it provides an alternative explanation for the continuity of the record. Clarify or drop.*

    We will change text to further incorporate the idea of a MBL ice dome. This was a hypothesis from several previous publications to explain geomorphological features in the eastern Ross Sea.

    Original Text (full paragraph provided for context):

"Geomorphological features on the Ross Sea bed do provide evidence of an expansive ice sheet which extended past Roosevelt Island during the LGM (Shipp et al., 1999; Anderson et al., 1984, 1992, 2014; Halberstadt et al., 2016). The stability of the Roosevelt Island ice dome and of Siple Dome implies that at this time, WAIS flowed around these sites rather than over them. This observation implies that as WAIS grew spatially, its thickness in the Ross Sea was limited, conditions that indicate ice streams were active throughout the last glacial period. Alternatively, Price et al. (2007) proposed that the geomorphological features observed in the eastern Ross Sea may represent building of an ice dome in Marie Byrd Land. The RICE records can not distinguish between these scenarios."

Revised Text:

"Geomorphological features on the Ross Sea bed do provide evidence of grounded ice north of Roosevelt Island during the LGM (Shipp et al., 1999; Anderson et al., 1984, 1992, 2014; Halberstadt et al., 2016). If these features were formed by an extended WAIS, it would imply that ice flowed around Roosevelt Island and Siple Dome and therefore must have been limited in its thickness. These conditions would indicate ice streams were active throughout the last glacial period. Alternatively, these geomorphic features may be the result of ice from a different origin. Price et al. (2007) proposed that during the LGM, an ice dome may have existed on Mary Byrd Land. In this scenario, thick, grounded ice could exist north of Roosevelt Island without flowing over or around the Roosevelt Island sea rise. The RICE records can not distinguish between these scenarios."

28. *Conclusions para 1: The fifth time we read this?*

    See response to Technical comment 9. We removed this.

29. *Many references found in the introduction do not come up again in the discussion. I'd suggest a bit more focus and continuity between the most relevant literature flowing from the intro to the discussion.*

    We agree with this comment and will reduce references which are only used in introduction.

30. *As a final point, it is tedious as a reviewer to have to spend so much time commenting on structure, something the author team could have worked on internally prior to submission. The age scale is important and should be presented as accessibly as possible.*

Responses to Reviewer 2:
First, Thank you for reviewing our manuscript. We agree with many of the suggestions made by reviewer 2. A number of these were in regard to improving organization and conciseness of the manuscript. This requires re-arranging sections and a significant number of edits at the sentence level. For brevity, we do not include every edit in our response to reviewer comments.
General Comments:

1. *This manuscript presents a suite of new gas records from an ice core drilled at Roosevelt Island, an ice rise in the Ross Sea. The primary objective is to establish its chronology by annual layer counting for relatively shallow depths and matching of gas records with existing WAIS Divide and Greenland ice core chronologies. The continuous part of the ice core extends to 65 kyr BP, suggesting that the Roosevelt Island has existed since at least this age. CH4 records show centennial-scale variability throughout the Holocene, with implications on natural vs. anthropogenic CH4 emission in pre-industrial periods. These discussions have some important implications for past climate and ice sheet variations. The dating method developed here is a nice contribution to the ice core community.*

   However, the lack of water isotope records and interpreted temperature records in this manuscript makes it difficult to review the estimated annual layer thickness using a firn densification model and its effects on dating and paleoclimatic implications. I find this study is potentially an important contribution to paleoclimatic communities but do not recommend publication in its current form. The authors would need to decide if they remove some parts of the manuscript regarding annual layer thickness estimates from firn modeling (but it will make the manuscript much less attractive), or they add water isotope data and temperature estimate (I would recommend the latter for publication in CP).

   The depth-age relationship, from which annual layer thickness is derived, is primarily dependent on the gas-based age constraints with only a small correction arising from the climate-dependent Δ-age. In this approach, temperature has only a secondary effect on annual layer thicknesses. One exception to this statement may be during the deglaciation when large changes in Δ-age are implied by rapid changes of δ^{15}N-N_2.

   We estimate past temperature based on the measurements of δD. The full high-resolution record of δD will be made publicly available in a forthcoming RICE project community paper led by project PI Nancy Bertler.

2. *The discussion of anthropogenic and natural CH4 variability needs some quantitative analyses (for example comparing frequency and variability after detrending for different time periods). To my eyes, the CH4 records appear to have different centennial-scale variations in earlier and later parts of the Holocene.*

   We have decided to remove this section (5.1 New observations of centennial-scale variability in the Holocene methane cycle) from the manuscript in response comments from reviewer 1. Content of this section is not discussed elsewhere in the paper and we hope that its removal will focus the paper on the other chronology-based conclusions and on the chronology development.

Specific comments:

1. *P5, L5. Regardless of the careful trimming of the ice in the same shape, the cut-bubble effect should change (generally decreasing) with depth due to the change in bubble sizes. The cut-bubble effect thus needs to be corrected.*

   We agree that the effect described by the reviewer should exist, but as we mentioned in the original text we have not made this correction to our total air content measurements because we do not believe that an accurate correction can be calculated for the RICE samples. This is because many of the RICE samples were fractured. Air intersecting a fracture may escape under vacuum and it is difficult to calculate the surface area of fractures. The air lost through fractures may be significantly greater than that lost due to sample preparation. To avoid samples with obviously large cut-bubble effects we excluded samples based on visual observations: samples with large fractures, with many fractures, which were comprised of multiple pieces of ice, or were an odd shape.

   However, we chose to include samples with small cracks in our data set. Small fractures are inconsistent in allowing air to escape. For this reason, it may not be possible to separate variations in TAC from gas loss through small fractures. In practice, small fractures can be hard to see which makes it possible for air to be lost through a fracture which was not observed.

   To clarify this issue we propose the following change in section 3.2 (P5, L3-9).

   Original text:

“Air trapped in bubbles, clathrates, or fractures intersecting the surface of the sample is lost, an effect called the cut-bubble effect (Martinerie et al., 1990). The cut-bubble effect is difficult to quantify, especially in ice which contains fractures through which air may be lost. No correction for the cut-bubble effect was applied to the TAC measurements presented here. Samples were cut to uniform shapes whenever possible to ensure that the cut-bubble effect was relatively constant in order to limit the influence it has on the variability of the TAC record. TAC analysis was rejected when the cut-bubble effect was believed to greatly impact the results, such as in samples which fractures could not be excluded or were excluded by cutting the sample into irregular shapes or into multiple pieces.”

New Text:

“The cut-bubble effect is difficult to quantify, especially in ice which contains fractures through which air may be lost. Samples were cut to uniform shapes whenever possible to ensure that the cut-bubble effect was relatively constant in order to limit the influence it has on the variability of the TAC record. However, many samples contained fractures through which air may be lost and greatly impact TAC. TAC data were rejected when gas loss was believed to greatly impact the results, such as in samples with fractures or samples which consisted of multiple pieces. However, small fractures were difficult to see and their contribution to gas loss is unknown. For this reason, we choose to not correct TAC measurements for the cut-bubble effect.”

2. *P16, L28. I do not understand why the temperature stability of the sample leads to the improvement in S/N of the gas chromatograph.*

   Insulation was added to the system as an attempt to minimize the water vapor in the headspace of our sample flasks (by decreasing the head space temperature) and to minimize variations of water vapor throughout the day. We also have made efforts to regulate the amount of ethanol in the chilled bath for the same purpose.

   We adjusted the sentence to clarify our intent and what we did.

   Original text (P16, L26-28):

   “Since Mitchell et al. (2013), insulation has been added around the ethanol bath and above where the flasks are mounted. The added insulation decreased the temperature variability of the ethanol bath and of the sample flasks throughout the day allowing for better measurement of pressure and improved signal-to-noise for the chromatograph.”

Edited text:

"Since Mitchell et al. (2013), insulation has been added around the ethanol bath and above where the flasks are mounted. The added insulation reduced the temperature and water vapor content of gas in the headspace of the flasks and decreased variability throughout the day. Both can affect methane measurements by changing the pressure reading or the retention time of methane in the GC column. Additionally, we have made efforts to more carefully regulate the amount of ethanol in the chilled bath and the temperature of hot water bath during melting. These steps improved stability of measurements and extraction between days."

3. *P17, L30. Please explain why the solubility correction factors are so different for sample and bubble-free ice?*

   The solubility corrections are empirically derived, so the difference in solubility between glacial sample ice and bubble-free ice is something we observe. We will add additional explanation to the supplement describing our theory about why our solubility results for bubble-free ice and glacial ice are different.

   We believe the difference results from the differences between how blank ice and ice containing air behave during melting.

   - Bubble-free ice melts slowly in comparison to glacial ice which sometimes melts rapidly and cracks violently. This, along with bubbles rising and breaching the meltwater surface, cause disturbances in the water-air interface and promotes exchange of CH_4 into the meltwater. This should lead to greater mixing and homogenization of air and water.
   - Bubbles released into the meltwater will be at higher pressures than the overlaying air because of surface tension. The higher partial pressure of CH_4 in those bubbles, in comparison to the standard gas added over the bubble-free ice, will cause air to go in to solution faster.
   - Because glacial ice tends to be melted sooner than blank ice, a longer time period for liquid-gas exchange is available.

4. *Fig. 2c and i. The scales of the axes should be the same for the left and right panels.*

   Done. Thank you for pointing this out.

5. *Fig. 5d. Why is the vertical line drawn at about 9000 yr BP and not near 9200 yr BP (highest occurrences)?*

   There is a difference between what we considered the "best" chronology and the most frequently occurring age of a specific depth. If we were to accept the most frequently occurring age of each sample depth in our Monte Carlo analysis as our final chronology, there is no guarantee that the age of ice increases with depth. Instead, we chose the age-scale with the best "goodness-of-fit." In this routine, goodness-of-fit is a single statistical value describing how similar both the CH_4 and $\delta^{18}O_{atm}$ records look like their corresponding records from WAIS Divide.

   Added text to be inserted before P8,L18:

   "The best age estimate of a sample depth (single point on the depth-age scale) is not necessarily the same as the most frequent age estimate for that depth. Fig. 5d shows in example from sample depth 621.28 m where there is a large difference between these two age estimates. In the case of sample depth 621.28 m, most realizations resulted in an age estimate of this sample of 9200 yr bP, similar to its prior age estimate of 9,240 yr bP, but the best realization estimated the age to be 9012 yr BP. The difference in estimates could be random because no significant improvement in the goodness-of-fit was found by adjusting the age of this depth or because shifting this age tended to worsen the fit of adjacent depths."

6. *Supplementary file "RICE17_Interpolated_Ages_20180530.txt" appears to contain two units for the ice age (probably C.E. and yr BP are switched at 343.5 m).*

   Corrected.

References

[Frieler et al. (2015)] Frieler, K., Clark, P. U., He, F., Buizert, C., Reese, R., Ligtenberg, S. R. M., Van Den Broeke, M. R., Winkelmann, R., and Levermann, A.: Consistent evidence of increasing Antarctic accumulation with warming, Nat. Clim. Change, 5, 348-352, https://doi.org/10.1038/nclimate2574, 2015.

[Fudge et al. (2016)] Fudge, T. J., Markle, B. R., Cuffey, K. M., Buizert, C., Taylor, K. C., Steig, E. J., Waddington, E. D., Conway, H., and Koutnik, M.: Variable relationship between accumulation and temperature in West

Antarctica for the past 31,000 years, Geophys. Res. Lett., 43, 3795-3803, https://doi.org/10.1002/2016GL068356, 2016.

[Winstrup et al. (2018)] Winstrup, M., Vallelonga, P., Kjær, H. A., Fudge, T. J., Lee, J. E., Riis, M. H., Edwards, R., Bertler, N. A. N., Blunier, T., Brook, E. J., Buizert, C., Ciobanu, G., Conway, H., Dahl-Jensen, D., Ellis, A., Emanuelsson, B. D., Keller, E. D., Kurbatov, A., Mayewski, P., Neff, P. D., Pyne, R., Simonsen, M. F., Svensson, A., Tuohy, A., and Wheatley, S.: A 2700-year annual timescale and accumulation history for an ice core from Roosevelt Island, West Antarctica, Clim. Past Discuss, https://doi.org/10.5194/cp-2017-101, in review, 2017.

List of changes made in the manuscript:
We have made a significant number of edits to the manuscript ranging from minor grammatical changes to restructuring of sections. Many of the changes are from suggestions of reviewers. Those changes are detailed with page and line numbers in the "Response to Reviewer" sections. Here we list other edits have been made:

- Page 1:
  - Lines 1-3: Condensed sentences to shorten abstract
  - Line 5: Removed references to "preliminary" results
  - Line 5-13: Condensed sentences to shorten abstract
  - Line 13-16: Removed reference to centennial scale variations of CH_4
- Page 2
  - Lines 2-27: Moved paragraphs 1 and 2 to a new section, section 2 "The Roosevelt Island ice core and glaciological history"
  - Line 28: Added text to introduce RICE project and to provide focus on chronology development:

    "The Roosevelt Island Climate Evolution Project (RICE) seeks to combine geophysical measurements with climate information from a well-dated ice core to improve constraints of the glacial history of the easter Ross Sea (Conway et al., 1999). With this motivation, the RICE project drilled and recovered a 763 m long ice core from Roosevelt Island. Here, we first present new data sets from the RICE ice core and then describe the development of the RICE17 age-scale, a composite age-scale which combines annual layer counts (Winstrup et al., 2017) with new age constraints and spans the top 753 m."
  - Line 28-32: Moved to section 2 "The Roosevelt Island ice core and glaciological history".
- Page 3
  - Line 1-13: Deleted text
  - Line 14: Added text:

    "The most precise chronologies for ice cores have been constructed by combining absolute age markers, such as volcanic ash layers, with annual layers counts from variations in chemical concentrations, stable isotope ratios of the ice, and electrical properties. Examples include the Greenlandic ice cores composite chronology (GICC05) which extends to 60 ka (Svensson et al., 2008) and the Antarctic WAIS Divide WD2014 chronology through the last 31 ka (Sigl et al., 2016). For the RICE ice core this strategy was only applicable above 165.02 m, the depth of the oldest absolute age marker, at 1251 C.E. (Winstrup et al., 2017). Annual layer interpretations were extended to 343.7 m (2649 yr BP, all ages are reported as years before present (BP), where present is defined as 1950 C.E.,Winstrup et al. 2017). Below this depth, annual layers became too thin to reliably interpret the seasonal signals.

For the 343.7-760 m section of the RICE ice core, the best age constraints are from measurements of methane and the isotopic composition of molecular oxygen ($\delta^{18}O_{atm}$). Variations in these parameters are globally synchronous (Bender et al., 1994; Blunier et al., 1998) meaning that, to a first-order, different ice cores will record the same atmospheric history. We establish the gas-phase depth-age relationship by matching the new RICE records to corresponding records from other ice cores with established chronologies. From the gas age-scale, an ice-phase age-scale was obtained by modeling the ice age-gas age offset (Δage). Δage is constrained by measurements of the isotopic composition of molecular nitrogen ($\delta^{15}N$-N_2) and estimates of temperature based on δD of ice. For overlapping depths the gas-based ice age estimates are in excellent agreement with the annual layer counted age estimates. A final age-scale for the entire core, named RICE17, is presented and is a composite of the annual layer-based age-scale for 0-343.7 m depth and the gas-based age-scale for deeper sections of the core."

  - Line 28: Inserted paragraphs 1 and 2 from page 2.

- Page 5

  - Line 4: Removed line 4-5

  - Line 4: Inserted discussion of cut bubble effect

    "In un-fractured ice, the cut-bubble correction can be estimated from the geometry of the sample and an estimate of bubble size. Ice samples were cut to uniform shapes to limit the variability in the measured TAC values related to geometry. However, inclusion of some fractures was often unavoidable and their contribution to gas loss is potentially large. For this reason we choose to not correct TAC measurements for the cut-bubble effect. TAC data were rejected when gas loss was believed to greatly impact the results, such as in samples with visible fractures or samples which consisted of multiple pieces."

- Line 12: Provided statistics for what we consider to be stable TAC throughout the record.
- Line 29: Added text:

  "In this section, we describe how the RICE17 age-scale is developed. We start with age constraints in the gas-phase based on well recorded variations in $\delta^{18}O_{atm}$ and methane. We then discuss how the gas age-scale is used to estimate the gas-phase ice-phase age offset and thus the ice age-scale. Finally, we compare the ice age-scale to the age-scale derived from annual layer interpretations."
- Line 29-Page 6 Line 26: Deleted

• Page 8

  - Line 18: Added text describing choice of final gas age-scale from matching algorithm:

    "We choose the best realization for gas age constraints for the RICE17 gas age-scale. The best age estimate (realization) is not necessarily the most frequent age estimate. Fig. 5d shows an example from sample depth 621.28 m where there is a large difference between these two age estimates. Large differences can occur because the prior age estimate (i.e. the age estimate based only on prior ACPs) differs by a large amount from the "true" age of that sample and because the goodness-of-fit parameter considers the fit over the whole record. For depth 621.28 m most realizations resulted in an age estimate of 9200 yr BP, similar to its prior age estimate of 9,240 yr BP, but the best realization estimated the age to be 9012 yr BP. There are two possible reasons for this type of result: 1) this realization is the best because it managed to push the age of this sample by ¿200 years towards younger ages while not significantly changing the ages of nearby sections which already fit well, or 2) no significant improvement in the goodness-of-fit was found by adjusting the age of this depth, and the goodness-of-fit was dictated by other sections of the record."

• Page 9

- Line 7-9: Added/replaced text to clarify building of target record from NGRIP CH_4 record:

  "Because NGRIP is in the northern hemisphere the methane concentration is higher than that in the RICE record. To account for this interpolar difference we scale the NGRIP target methane record (Baumgartner et al., 2014) to Antarctic values using an empirical least squares fit between WAIS and NGRIP records between 55-67.8 ka."
- Line 12-19: Many smaller edits for clarity
- Line 32: Added sentence describing Figure 6:

  "The left panel of Fig. 6 shows the data as a function of depth, color-coded by age. The right panel shows the reconstructed time history of these variables, color-coded by depth."

- Page 10
  - Line 13-18: Deleted
- Page 11
  - Line 33: Added text:

    "The sensitivity tests include a wide range of temperature histories to account for the possibility that some variations in δD were caused by non-thermal effects such as variability in precipitation seasonality, moisture sources and pathways, and post-depositional vapor exchange."
- Page 12
  - Line 27-Page 13 Line 15: Deleted Section 5.1 "New observations of centennial-scale variability in the Holocene methane cycle"
- Page 13
  - Line 17-19: Condensed sentences
  - Line 28: Added text:

    " This feature is not apparent in other ice cores from the Ross Sea region, but those records tend to be difficult to interpret because of chronological uncertainties, such as is the case for Taylor Dome (Baggenstos et al., 2017), or because of unexplained jumps in δ^{15}N-N_2, such as is the case for Siple Dome (Severinghaus et al., 2009)"

- Line 33: Added text for context:

  "Analysis of the lead-lag relationship between methane and the thermal-signal from δ^{15}N-N_2 has been used to infer a closely coupled climate throughout the tropics and northern hemisphere (Rosen et al., 2014). These climate events are believed to originate in the northern hemisphere and propagate to the southern hemisphere (Blunier et al., 1998; Blunier and Brook, 2001; Buizert et al., 2015a)."

- Page 14
  - Line 5-30: Edited text following suggestions from reviewers. These two paragraphs discuss possible explanations for a large and abrupt decrease in δ^{15}N-N_2. Revisions were made for clarity and to emphasize our preferred explanation.

- Page 16
  - Line 7-14: Removed text referencing anthropogenic contributions to centennial scale variations of CH_4
  - Line 28: Added text:

    " The added insulation reduced the temperature and water vapor content of gas in the headspace of the flasks and decreased their variability. Both can affect methane measurements by changing the pressure reading or the retention time of methane in the GC column. We also made efforts to more carefully regulate the amount of ethanol in the chilled bath and temperature of the hot water bath during melting. These steps improved stability of measurements and extraction between days."

- Page 32
  - Corrected figure for sub-plot labels

- Page 34
  - Changed axis label from "sample resolution" to "sample spacing"

- Page 36
  - Minor changes to caption

- Page 38

- Added panel to figure which shows CH_4 data for comparison with δ^{15}N-N_2 data.

An 83,000 year old ice core from Roosevelt Island, Ross Sea, Antarctica

James E. Lee[1], Edward J. Brook[1], Nancy A. N. Bertler[2,3], Christo Buizert[1], Troy Baisden[3,4], Thomas Blunier[5], V. Gabriela Ciobanu[5], Howard Conway[6], Dorthe Dahl-Jensen[5], T. J. Fudge[6], Richard Hindmarsh[7], Elizabeth D. Keller[3], Frédéric Parrenin[8], Jeffrey P. Severinghaus[9], Paul Vallelonga[5], Edwin D. Waddington[6], and Mai Winstrup[5]

[1]College of Earth, Ocean, and Atmospheric Sciences, Oregon State University, Corvallis, OR 97331, USA
[2]Antarctic Research Centre, Victoria University of Wellington, Wellington, New Zealand
[3]GNS Science, Gracefield, Lower Hutt, 5010, New Zealand
[4]Now at Faculty of Science and Engineering, University of Waikato, Hamilton, New Zealand
[5]Centre for Ice and Climate, Niels Bohr Institute, University of Copenhagen, Copenhagen, Denmark
[6]Department of Earth and Space Sciences, University of Washington, Seattle, WA 98195, USA
[7]British Antarctic Survey, Cambridge CB3 0ET, United Kingdom
[8]University Grenoble Alpes, Centre National de la Recherche Scientifique, Institut de Recherche pour le Développement, Institut des Géosciences de l'Environnement, 38000 Grenoble, France
[9]Scripps Institution of Oceanography, University of California, San Diego, La Jolla, CA 92093, USA

Correspondence: James E. Lee (JLee@COAS.OregonState.edu)

Abstract. In 2013~~,~~ an ice core was recovered from Roosevelt Island, an ice dome between two submarine troughs carved by paleo-ice-streams in the Ross Sea, Antarctica~~, as part of the Roosevelt Island Climate Evolution (RICE) project. Roosevelt Island is located between two submarine troughs carved by paleo-ice-streams.~~ The ice core is part of the Roosevelt Island Climate Evolution (RICE) project and ~~The RICE ice core~~ provides new ~~important~~ information about the past configuration of the West Antarctic Ice Sheet and its retreat during the ~~most recent~~ last deglaciation. In this work, we present the RICE17 chronology, which establishes the depth-age relationship for the top 753 m of the 763 m core. ~~and discuss preliminary observations from the new records of methane, the isotopic composition of atmospheric molecular oxygen ($\delta^{18}O_{atm}$), the isotopic composition of atmospheric molecular nitrogen ($\delta^{15}N$-N_2), and total air content (TAC).~~ RICE17 is a composite chronology combining annual layer interpretations for 0-343 m (Winstrup et al., 2017), with new estimates for gas and ice ages based on synchronization of methane and $\delta^{18}O_{atm}$ records to corresponding records from the WAIS Divide ice core and by modeling of the gas age-ice age difference.~~, gas synchronization, and firn modeling strategies in different sections of the core. An automated matching algorithm is developed for synchronizing the high-resolution section of the RICE gas records (60-720 m, 1971 CE to 30 ka) to corresponding records from the WAIS Divide ice core, while deeper sections are manually matched. Ice age for the top 343 m (2635 yr BP, before 1950 C.E.) is derived from annual layer interpretations and described in the accompanying paper by Winstrup et al. (2017). For deeper sections, the RICE17 ice age scale is based on the gas age constraints and the ice age-gas age offset estimated by a firn densification model.~~

Novel aspects of this work include: 1) an automated algorithm for multi-proxy stratigraphic synchronization of high resolution gas records ~~stratigraphic matching of centennial-scale variations in methane for pre-anthropogenic time periods, a strategy~~

~~which will be applicable for developing precise chronologies for future ice cores~~, 2) ~~the observation of~~ synchronization using centennial-scale variability in methane for pre-anthropogenic time periods (60-720 m, 1971 CE to 30 ka), a strategy applicable for future ice cores ~~throughout the Holocene which suggests that similar variations during the late pre-industrial period need not be anthropogenic~~, and 3) the observation of continuous climate records dating back to ∼65 ka providing ~~which provide~~ evidence that the Roosevelt Island Ice Dome was a constant feature throughout the last glacial period.

1 Introduction

[1]~~The stability of the West Antarctic Ice Sheet (WAIS) is one of the largest uncertainties in predicting future sea level rise (Church et al., 2013; Church et al., 2014; Church et al., 2014; Church et al., 2015; Church et al., 2016). Much of the ice sheet is grounded below sea level with the bed deepening towards the center of the ice sheet. If the ice sheet were to retreat, the grounding line would move to deeper water depths where it is physically less stable (a phenomenon known as marine ice sheet instability, Hughes 1973; Hughes 1974; Hughes 2007; Hughes 2015) and more vulnerable to undercutting by "warm" subsurface currents (Robin and Adie, 1964; Robin and Adie, 2004) and ice cliff instability (DeConto and Pollard, 2016) promoting enhanced ice flow and further mass loss. Vulnerability of WAIS to future warming can be assessed by investigating how it has responded to different climate regimes in the past. Unfortunately, geologic evidence of the past size and extent of Antarctic ice sheets is spatially sparse, tends to have large chronological uncertainty, and is sometimes contradictory (Whitehouse et al., 2012; Whitehous~~

[2]~~The Ross Embayment is the largest drainage of WAIS, both in terms of area and mass loss (Halberstadt et al., 2016). The glacial history of WAIS in the Ross Sea has been speculated about since Captain James Ross first mapped its edge in 1841-1842, followed by the first geologic studies of the region during the Discovery, Nimrod, and Terra Nova expeditions (Scott, 1907; Scott, 1910-11; Scott, 1921). In the modern era, two basic scenarios have been proposed for the configuration of WAIS in the Ross Embayment during the Last Glacial Maximum (LGM) (Stuiver et al., 1981). First, in the "maximum scenario," a thick and grounded ice sheet in the Ross Sea extended to the continental shelf break (Denton et al., 1989). Details of this scenario are supported by geomorphic features including grounding-zone wedges, which form at the terminus of marine based glaciers (Shipp et al., 1999), and over-compressed diamictons, which are the result of thick overlying ice (Anderson et al., 1984, 1992). Evidence of high stands in the Transantarctic Mountains and the islands of the western Ross Sea (Denton and Marchant, 2000) as well as cosmogenic exposure dates on nunataqs in Marie Byrd Land (Stone et al., 2003) also support this idea. In an alternate scenario, Denton et al. (1989) proposed that grounded ice in the Ross Sea was kept thin by fast-flowing ice streams. In this scenario, the retreat of WAIS during the last deglaciation may not have contributed significantly to sea level change. Studies of ice cores from Byrd Station (Steig et al., 2001) and Siple Dome (Waddington et al., 2005), glacial modeling (Parizek and Alley, 2004), and cosmogenic exposure dates from the Ohio Range (Ackert et al., 1999, 2007) all support this "minimal scenario."~~

[1]Paragraph moved to new section "The Roosevelt Island ice core and glaciological history"

[2]See footnote 1

The Roosevelt Island Climate Evolution Project (RICE) seeks to combine geophysical measurements with climate information from a well-dated ice core to improve constraints of the glacial history of the easter Ross Sea (Conway et al., 1999). With this motivation, the RICE project drilled and recovered a 763 m long ice core from Roosevelt Island. Here, we first present new data sets from the RICE ice core and then describe the development of the RICE17 age-scale, a composite age-scale which combines annual layer counts (Winstrup et al., 2017) with new age constraints and spans the top 753 m. ~~In 2013, an ice core was drilled at the divide of Roosevelt Island as part of the Roosevelt Island Climate Evolution (RICE) project. Roosevelt Island is an ice dome located on a submarine plateau (~200 mbsl) dividing the Whales Deep and Little America Basins in the eastern Ross Sea (Fig. 1). During the LGM, these troughs were presumably occupied by the extension of the modern Bindschadler and MacAyeal ice streams (Ice Streams D and E, respectively) (Shipp et al., 1999), and Roosevelt Island would have been located along the main ice flow of WAIS. One motivation for the RICE project was to acquire a well-dated ice core that could be used in combination with geophysical measurements to unravel the glacial history of the eastern Ross Sea (Conway et al., 1999; Conway et al., 2018, *personal communication*).~~

~~In this paper we first present measurements of methane, the isotopic composition of molecular oxygen ($\delta^{18}O_{atm}$), the isotopic composition of molecular nitrogen ($\delta^{15}N\text{-}N_2$), and total air content (TAC). We use these datasets to establish the RICE17 chronology for the deeper section of the RICE ice core, a composite chronology combining annual layer interpretations (Winstrup et al., 2017), gas synchronization, and modeling of the ice age-gas age offset. The gas age-scale was synchronized by (1) an automated matching routine, adapted from Huybers and Wunsch (2004) and novel in the application to ice cores, which simultaneously matched methane and $\delta^{18}O_{atm}$ records from RICE to records from the WAIS Divide ice core on the WD2014 age-scale (0-720 m, present-30 ka), (2) by visual matching to records from WAIS Divide for the lower-resolution section (720-746 m, 30-64.6 ka), and (3) by visual matching to records from the NGRIP ice core on a modified GICC05modelext chronology for ages older than WD2014 (746-752.95 m, 64.6-83 ka). Ice below 753 m is highly thinned, potentially disturbed and the gas age could not be identified. The RICE17 ice age-scale for the top 343.7 m (2649 yr BP, before 1950 C.E.) is based on annual layer interpretations (Winstrup et al., 2017). Below this depth, ice age was derived from the gas age-scale by adding the ice age-gas age offset, estimated with a dynamic firn densification model (firn is the the upper layer of an ice sheet where snow compacts and transforms into ice, Buizert et al. 2015).~~

The most precise chronologies for ice cores have been constructed by combining absolute age markers, such as volcanic ash layers, with annual layers counts from variations in chemical concentrations, stable isotope ratios of the ice, and electrical properties. Examples include the Greenlandic ice cores composite chronology (GICC05) which extends to 60 ka (Svensson et al., 2008) and the Antarctic WAIS Divide WD2014 chronology through the last 31 ka (Sigl et al., 2016). For the RICE ice core this strategy was only applicable above 165.02 m, the depth of the oldest absolute age marker, at 1251 C.E. (Winstrup et al., 2017). Annual layer interpretations were extended to 343.7 m (2649 yr BP, all ages are reported as years before present (BP), where present is defined as 1950 C.E.,Winstrup et al. 2017). Below this depth, annual layers became too thin to reliably interpret the seasonal signals.

For the 343.7-760 m section of the RICE ice core, the best age constraints are from measurements of methane and the isotopic composition of molecular oxygen ($\delta^{18}O_{atm}$). Variations in these parameters are globally synchronous (**?**Blunier et al., 1998) meaning that, to a first-order, different ice cores will record the same atmospheric history. We establish the gas-phase depth-age relationship by matching the new RICE records to corresponding records from other ice cores with established chronologies. From the gas age-scale, an ice-phase age-scale was obtained by modeling the ice age-gas age offset (Δage). Δage is constrained by measurements of the isotopic composition of molecular nitrogen (δ^{15}N-N_2) and estimates of temperature based on δD of ice. For overlapping depths the gas-based ice age estimates are in excellent agreement with the annual layer counted age estimates. A final age-scale for the entire core, named RICE17, is presented and is a composite of the annual layer-based age-scale for 0-343.7 m depth and the gas-based age-scale for deeper sections of the core.

The approach used ~~to develop the~~ for RICE17 ~~age-scale~~ is not unique ~~for deep ice cores (Buizert et al., 2015),~~ but includes several refinements that improve dating accuracy~~of the chronological techniques in order to improve the dating accuracy~~. Primarily, the RICE17 chronology benefited from the availability of high-resolution gas records from both the RICE ice core and the WAIS Divide ice core. Centennial-scale variability of methane was well-captured ~~in both the RICE and WAIS Divide ice core~~ for the last 30 ka in both data sets~~, a mode of variability previously limited for synchronization to the late Preindustrial Holocene due to the resolution of available records (Mitchell et al., 2011, 2015)~~. Additionally, an automated matching routine, adapted from Huybers and Wunsch (2004) and novel in the application to ice cores, simultaneously matched methane and $\delta^{18}O_{atm}$ records for ice up to 30 ka (0-720 m). ~~The simultaneous matching of high-resolution records of methane and $\delta^{18}O_{atm}$ increased the strength of gas age constraints~~The multi-proxy approach to synchronization leads to strengthened age estimates. ~~Finally, synchronization by an automated matching algorithm allowed for refinement of the age-scale with a Monte Carlo approach.~~Using an automated routine resulted in a more objective match of the RICE gas records to the reference records and a Monte Carlo based estimate of age uncertainty.

RICE17 is a continuous chronology with age monotonically increasing with depth~~, absent of discontinuities and with monotonically increasing age with depth,~~ until at least 64.6 ka. At 746.00 m folding of the ice is observed and the age-scale is segmented and no longer continuous. The oldest ice ~~age~~ near the bottom of the core has a minimum of 83 ka. ~~All ages are reported as years before present (BP), where present is defined as 1950 C.E.~~ We use these observations, in support with measurements of total air content (TAC) to interpret that the Roosevelt Islnd ice dome was stable throughout the last glacial maximum.

2 The Roosevelt Island ice core and glaciological history

Understanding the stability of the West Antarctic Ice Sheet (WAIS) is important for predicting future sea level rise (Church et al., 2013; Jevrejeva et al., 2014; Golledge et al., 2014; Pollard et al., 2015; DeConto and Pollard, 2016). Much of the ice sheet is grounded below sea level with the bed deepening towards the center of the ice sheet. This configuration is thought to be unstable and prone to rapid disintegration due to physical forces (Hughes, 1973; Weertman, 1974; Schoof, 2007; Feldmann and Levermann, 2015)), vulnerability to undercutting by “warm” subsurface currents (Robin and Adie, 1964; Shepherd et al., 2004), and ice cliff instability (DeConto and Pollard, 2016). Vulnerability of WAIS to future warming can be assessed by investigating how it has responded to different climate regimes in the past. Unfortunately, geologic evidence of the past size and extent of Antarctic ice sheets is spatially sparse, tends to have large chronological uncertainty, and is sometimes contradictory (Whitehouse et al., 2012; Anderson et al., 2014; Bentley et al., 2014; Clark and Tarasov, 2014; Halberstadt et al., 2016; McKay et al., 2016).

The Ross Embayment is the largest drainage of WAIS, both in terms of area and mass loss (Halberstadt et al., 2016). Historically, two basic scenarios have been proposed for the configuration of WAIS in the Ross Embayment during the Last Glacial Maximum (LGM) (Stuiver et al., 1981). In the “maximum scenario,” a thick and grounded ice sheet in the Ross Sea was hypothesized to extend to the continental shelf break (Denton et al., 1989). Details of this scenario are supported by geomorphic features including grounding-zone wedges, which form at the terminus of marine based glaciers (Shipp et al., 1999), and over-compressed diamictons, which are the result of thick overlying ice (Anderson et al., 1984, 1992). Evidence of high stands in the Transantarctic Mountains and the islands of the western Ross Sea (Denton and Marchant, 2000) as well as cosmogenic exposure dates on nunataqs in Marie Byrd Land (Stone et al., 2003) also support this idea. In an alternate scenario, Denton et al. (1989) proposed that grounded ice in the Ross Sea was kept thin by fast-flowing ice streams. In this scenario, the retreat of WAIS during the last deglaciation may not have contributed significantly to sea level change. Studies of ice cores from Byrd Station (Steig et al., 2001) and Siple Dome (Waddington et al., 2005), glacial modeling (Parizek and Alley, 2004), and cosmogenic exposure dates from the Ohio Range (Ackert et al., 1999, 2007) all support this “minimal scenario.”

Roosevelt Island is an ice dome located in the eastern Ross Sea in West Antarctica (79.36° S, 161.71° W; elev. 550 m above sea level, Fig. 1) It is grounded on a submarine plateau (∼200 mbsl) dividing the Whales Deep and Little America Basins. During the LGM these troughs were presumably occupied by the extension of the modern Bindschadler and MacAyeal ice streams (Ice Streams D and E, respectively) (Shipp et al., 1999), and Roosevelt Island would have been located along the main ice flow of WAIS.

The 763 m long RICE ice core was drilled to bedrock near the summit of Roosevelt Island~~, in the eastern Ross Sea in West Antarctica (79.36° S, 161.71° W; elev. 550 m above sea level, Fig. 1)~~. In addition to the main deep core, a shallow core was drilled to 20 m and several snow pits were sampled to understand recent climate (Bertler et al., 2018). Local mean annual air temperature is -23.5° C and annual snow accumulation is estimated to be ∼0.22 m ice equivalent, based on annual layers in snow pits (Bertler et al., 2018). A cooler estimate of modern temperature, -27.4 ± 2.4° C based on ERA interim data from 1979-2012, was presented in Bertler et al. (2018), but this estimate is cooler than borehole thermometry measurements and previously published estimates for Roosevelt Island (Herron and Langway, 1980; Conway et al., 1999; Martín et al., 2006) and does not provide a good fit to the density profile in the firn model. Other estimates of recent accumulation at the RICE drill site range from 0.18 m ice per year to 0.27 m ice per year, depending on method and time period (Winstrup et al., 2017; Bertler et al., 2018; Herron and Langway, 1980; Conway et al., 1999; Kingslake et al., 2014).

3 New data sets from the RICE ice core

3.1 Methane measurements

The RICE discrete methane record was measured at Oregon State University (OSU) following methods described by Mitchell et al. (2011, 2013) with updates described in Appendix A. A total of 702 samples were measured at 583 distinct depths between 60-753 m (Fig. 2a, e). Samples from 406 depths were measured between 60 and 670 m, dating from ∼1970 C.E. to 11.87 ka, with a mean sample spacing of 28.75 years. Between 670 and 718.13 m the record spans 11.87 to 29.9 ka; 96 samples in this interval provide age resolution of 189 years. Age resolution decreases significantly for deeper depths. The interval from 718.53 to 746.00 m corresponds to 30.1-64.6 ka and the methane record has a mean resolution of 548 years. The deepest dated ice is at 752.95 m and has an age of 83 ka (±2 ka).

Methane was also measured continuously with a laser spectroscopy technique (Stowasser et al., 2012; Rhodes et al., 2013) during two separate continuous flow analysis (CFA) campaigns at GNS Science (Gracefield, New Zealand) in 2013 and 2014 (Pyne et al., 2018). The CFA methane record was affected by variability of air flow to the measurement instrument and fractures within the core which that allowed drill fluid and modern air into the melt head. Exclusion of these artifacts caused significant gaps in the record, particularly at depths below 676 m (12.6 ka). We consider the CFA methane record to be a supplement to the more robust but lower resolution discrete data set. Between 29.9-59.1 ka, the CFA methane record is critical for establishing age control. Below ∼746 m (64.6 ka), the CFA methane record is data are difficult to interpret because of gaps in the record, uncertainty in measurement depth, and uncertainty in the methane calibration of CH_4 (Appendix B).

Several anomalously high discrete methane measurements appear between 44.6-50.9 ka (729.05-736.05 m) and below 64.6 ka (746 m) (Fig. 3a). In the former interval, methane is enriched by ∼30 ppb compared with the WAIS Divide CFA data methane record (Rhodes et al., 2015). Many samples in this section included This is likely due to healed fractures which can enclose include modern air in the ice sample if they heal (Aydin et al., 2010). All RICE ice core samples deeper than 500 m were visually inspected for fractures as they were prepared for measurement and for drill fluid during extraction. In fractured ice it was common to see drill fluid in the flask as the samples were melted for gas extraction. However, neither observation was a strong indicator that a sample would have an elevated methane concentration. None of these high concentration results were rejected.

3.2 Total air content measurements

Total air content (TAC) is defined as the amount of air trapped in a sample per gram of ice in units of cm^3 air at STP/g ice. TAC (Fig. 2d, h) was measured at OSU as part of the methane concentration measurement following methodology of Mitchell et al. (2015) and updates from Edwards et al. (in prep). TAC is influenced by accumulation and temperature, seasonal gradients in the firn related to total summer insolation (Raynaud et al., 2007), thermal gradients in the firn from multi-annual climate trends, and surface air pressure (Martinerie et al., 1992; Raynaud and Whillans, 1982).

Air trapped in bubbles, clathrates, or fractures intersecting the surface of the sample is lost, The measured TAC is typically corrected for loss of air from bubbles which intersect the surface of the sample, an effect called the cut-bubble effect (Martinerie et al., 1990). In un-fractured ice, the cut-bubble correction can be estimated from the geometry of the sample and an estimate of bubble size. Ice samples were cut to uniform shapes to limit the variability in the measured TAC values related to geometry. However, inclusion of some fractures was often unavoidable and their contribution to gas loss is potentially large. For this reason we choose to not correct TAC measurements for the cut-bubble effect. ~~The cut-bubble effect is difficult to quantify, especially in ice which contains fractures through which air may be lost. No correction for the cut-bubble effect was applied to the TAC measurements presented here. Samples were cut to uniform shapes whenever possible to ensure that the cut-bubble effect was relatively constant in order to limit the influence it has on the variability of the TAC record.~~ TAC ~~analysis was~~ data were rejected when gas loss ~~the cut-bubble effect~~ was believed to greatly impact the results, such as in samples ~~which~~ with visible fractures ~~could not be excluded~~ or ~~were excluded by cutting the sample into irregular shapes or into~~ which consisted of multiple pieces. Of the 706 samples measured at OSU for TAC, 165 results were rejected based upon visual inspection of the sample. Many of these came from the 670-752.95 m (11.7-83 ka) interval where only 58 of 177 TAC measurements are considered reliable. Nonetheless, the TAC record from the RICE ice core appears remarkably consistent (age weighted mean = 0.1182 cm^3 air-STP/g ice, age weighted standard deviation = 0.0023 cm^3 air-STP/g ice, n=410, Fig. 3d).

3.3 $\delta^{18}O_{atm}$ and $\delta^{15}N$-N_2 measurements

$\delta^{18}O_{atm}$ and $\delta^{15}N$-N_2 were measured on samples adjacent to the discrete methane samples (Fig. 2b, f and c, g, respectively). Analysis was conducted at Scripps Institution of Oceanography following Petrenko et al. (2006) and Severinghaus et al. (2009). Pooled standard deviation of replicate measurements ~~for $\delta^{18}O_{atm}$~~ is 0.006‰ for $\delta^{18}O_{atm}$ and ~~for $\delta^{15}N$-N_2~~ is 0.0027‰ for $\delta^{15}N$-N_2 (both scales are relative to modern atmospheric composition).

Variations of $\delta^{18}O_{atm}$ are primarily caused by changes in location and intensity of low-latitude rainfall that affect the $\delta^{18}O$ of leaf water used in photosynthesis (Severinghaus et al., 2009; Landais et al., 2007; **?**) (Seltzer et al., 2017) and changes in seawater $\delta^{18}O$ caused by ice sheets on glacial cycles (Horibe et al., 1985; Bender et al., 1985, 1994; Sowers et al., 1993). Importantly, these variations are well known in independently dated ice cores and the atmosphere is well mixed on the relevant timescales, so $\delta^{18}O_{atm}$ variability may be used as a chronostratigraphic marker (Bender et al., 1994). These variations are well sampled in the RICE record until ∼64.6 ka (746.00 m), beyond which the chronology is no longer continuous.

~~Molecular~~ Atmospheric N_2 ~~in the atmosphere~~ is isotopically stable over very long time-scales (Hattori, 1983; Sowers et al., 1989). Variability of $\delta^{15}N$-N_2 in the ice core record primarily reflects changes in gravitational fractionation and thermal fractionation within the firn ~~which primarily result from~~ due to changes in surface temperature and accumulation rate (Schwander, 1989; Sowers et al., 1989).

4 Strategy for developing the chronology

In this section, we describe how the RICE17 age-scale is developed. We start with age constraints in the gas-phase based on well recorded variations in $\delta^{18}O_{atm}$ and methane. We then discuss how the gas age-scale is used to estimate the gas-phase ice-phase age offset and thus the ice age-scale. Finally, we compare the ice age-scale to the age-scale derived from annual layer interpretations.

All age control points (ACPs), additional control points from the synchronization routine (floating control points, discussed below) and gas adn ice ages interpolated to more closely spaced depths are provided in the supplementary material.

Annual layer counting strategies have been used to construct some of the most precise chronologies for ice cores, for example the Greenlandic ice cores composite chronology (GICC05) which extends to 60 ka (Svensson et al., 2008) and the Antarctic WAIS Divide WD2014 chronology which is dated with annual layer interpretations through the last 31 ka (Sigl et al., 2016). Annual layer counting for the RICE ice core provided a timescale to 343.7 m depth, extending to 2649 yr BP (Winstrup et al., 2017), using Straticounter, a multi-proxy automated layer counting algorithm (Winstrup et al., 2012; Winstrup et al., 2016). For the RICE ice core, below the most recent 100 years annual layers were interpreted from variations in pH, dust, black carbon, Ca^{+2}, and conductivity with a further constraint from a single absolute age marker at 165.02 m depth corresponding to 1251 C.E. (Winstrup et al., 2017).

No absolute age markers were found prior to 1251 C.E. and annual layers are too thin to distinguish prior to 2649 yr BP. The best chronological constraints for this section are measurements of methane and $\delta^{18}O_{atm}$, which we use to synchronize RICE with corresponding records from other ice cores with established chronologies. The RICE records are synchronized in four different sections. (1) Between present and 11.7 ka (48-670 m) and (2) from 11.7-30.66 ka (670-719.3 m), an automated synchronization routine was used to value match methane and $\delta^{18}O_{atm}$ records from RICE and WAIS Divide ice cores (Section 4.1). Separating these two time periods allowed for a better match for the 0-11.7 ka section, where sample resolution was better and variations of atmospheric methane were smaller (Fig. 3). (3) For the interval between 30.66 and 64.6 ka (719.30-746.00 m), a set of age control points (ACPs) were visually chosen to match methane and $\delta^{18}O_{atm}$ records from the RICE ice core to records from the WAIS Divide ice core on the WD2014 chronology (Table 1). (4) The discontinuous section, below 746 m (64.6 ka), is beyond the age of the WAIS Divide ice core, and target records for methane and $\delta^{18}O_{atm}$ were developed from records from the NGRIP ice core (Landais et al., 2007; Landais et al., 2014) (Section 4.2). A modification was made to the GICC05modelext age-scale for NGRIP (Wolff et al., 2010; Wolff et al., 2014) for consistency with the WD2014 chronology (Section 4.2).

An ice age-scale for RICE was obtained by adding Δage to the gas ages. Δage is estimated using a dynamic firn densification model (Buizert et al., 2015) constrained by past lock-in depth (LID) determined from $\delta^{15}N\text{-}N_2$, temperature determined from δD (Bertler, 2018, *personal communication*) and borehole temperature (Bertler et al., 2018; Bertler et al., Unpublished). Description of the Δage model is provided in Section 4.4.

As discussed above, the final RICE17 ice age-scale merges the annual layer counts and the gas-derived ice age-scale developed here. Good agreement between the two ice age-scales obviates any need to adjust either chronology at the transition depth. This strategy respects the higher resolution and lower uncertainty of the annual layer interpretations of ice age. The ACPs, additional control points from the synchronization routine (floating control points, discussed below), and gas and ice ages in RICE17 for evenly spaced depths are provided in the supplementary material.

4.1 An automated matching algorithm for synchronizing ice core records: 0-30 ka

~~For the purpose of synchronizing between gas records, a~~An automated matching algorithm was adapted from Huybers and Wunsch (2004) to synchronize between gas records. ~~The method starts with a set of p~~Prior ACPs, shown as open triangles in Fig. 5, ~~which~~ all correspond to well defined ~~variations in~~ increases or decreases of either methane or $\delta^{18}O_{atm}$ ~~(Table 1)~~. ~~Age uncertainty of ACPs was estimated from the length of time~~ We assume that the uncertainty (2 standard deviations) for an ACP corresonds to the time elapsed between 25% and 75% of the change in either methane or $\delta^{18}O_{atm}$ (Table 1) ~~the observed change of relevant variable~~. The goal of the routine is to iteratively adjust the interpolation between ACPs to improve a goodness-of-fit parameter by following steps 1-9 described below.

"Goodness-of-fit" is calculated as the χ^2 value comparing the normalized methane record from the RICE ice core to expectant values interpolated from the WAIS Divide ice core plus the analagous χ^2 value comparing the normalized $\delta^{18}O_{atm}$ records. The algorithm can accept additional parameters for synchronization, such as CO_2 or N_2O, if available ~~but methane and $\delta^{18}O_{atm}$ are currently the only two suitable parameters available for the RICE ice core~~. In this analysis, we ~~have~~ normalized both the methane and $\delta^{18}O_{atm}$ records to have the same mean (5) and variance (1) in order to equally weight their χ^2 values and their importance to the synchronization.

A realization starts by randomly perturbing the age of ACPs within their prescribed uncertainty (Table 1) to define an initial depth-age scale. The perturbed ACPs remain fixed throughout the realization. ACPs are given the subscript k, where k=1 is the youngest/shallowest ACP. The records are then broken into N subsections which are distributed between ACPs. Subsections are designated with a subscript i, where i=1,2,3,...N. Floating control points (FCPs) are defined as the bounding depths/ages of these subsections, which will include the initial ACPs. Prior to any perturbations, the durations of the subsections (Δt) are approximately the same. We have chosen Δt to roughly match the recurrence interval of variations of methane in the reference record and so that each subsection contains about five methane and five $\delta^{18}O_{atm}$ samples. The following steps are repeated to optimize goodness-of-fit:

1. Random scaling factors (p_i), which perturb the durations of the subsections, are drawn for each subsection from a normal distribution of μ=1 and σ_1=0.25.

$$\Delta \mathrm{t}'_i = \Delta \mathrm{t}_i \cdot p_i$$

2. Because random perturbations will change the length of time between the initial ACPs, we apply a second scaling so the perturbed chronology remains consistent with the prior ACPs. In this case, ACP_k and ACP_{k+1} are the nearest gas ACPs bounding subsection i, respectively. ACP' is the perturbed age of the gas age constraint after step 1, and $\Delta \mathrm{t}^*_i$ is the duration of the subsection after the second scaling:

$$\Delta \mathrm{t}^*_i = \Delta \mathrm{t}'_i \cdot \left(\frac{\mathrm{ACP}_{k+1} - \mathrm{ACP}_k}{\mathrm{ACP}'_{k+1} - \mathrm{ACP}'_k}\right)$$

3. Mean "accumulation rate" of each subsection ($\overline{A}_i$) is calculated following Nye (1963), which assumes that the thickness of annual layers ($\overline{\lambda}_i$) is the product of their original thickness and their relative depth ($\frac{\overline{z}_i}{H}$):

$$\overline{A}_i = \overline{\lambda}_i \cdot (1 - \frac{\overline{z}_i}{H})^{-1}$$

where $\overline{z}_i$ is the mid-depth of the subsection i, H is the thickness of the ice sheet, and both $\overline{z}_i$ and H are in ice equivalent units.

Because the assumptions about thinning from Nye (1963) is too simple to describe the flow conditions at Roosevelt Island, we do not consider this result to be representative of the true accumulation history. The assumption is necessary for the purposes of interpolating age versus depth to ensure that annual layer thickness decreases smoothly between FCPs. An accumulation history that we believe is more accurate is calculated below with an alternative method, using a dynamic firn model (Section 4.4).

4. A perturbed chronology is only accepted if:

   (a) Intervals between FCPs (Δt_i^*) are within a factor of 10 of the initial durations,

   $$\frac{1}{10} \cdot \frac{(t_{end}-t_1)}{N} < \Delta t_i^* < 10 \cdot \frac{(t_{end}-t_1)}{N}$$

   (b) Mean "accumulation rates" are realistic ($\overline{A}_i$ >0 cm ice eq per yr, $\overline{A}_{max} < 75$ cm ice eq per yr), and

   (c) Mean "accumulation rates" of adjacent subsections are within a factor of 2 of each other.

   These conditions provide loose restrictions for continuity in the depth-age relationship although they may not be physically realistic for the site.

5. Ages for all RICE sample depths are interpolated from the perturbed FCPs (Step 3), assuming piece-wise constant accumulation between FCPs and a linearly decreasing thinning function (Nye, 1963).

6. Goodness-of-fit is calculated on the perturbed age-scale (goodness-of-fit = $\chi^2_{CH4} + \chi^2_{\delta 18Oatm}$).

7. When a perturbation improves the goodness-of-fit, that iteration becomes the base for subsequent perturbations.

8. The cycle is repeated until 20 sequential perturbations fail to improve the goodness-of-fit in step 6.

9. Starting with the FCPs from step 8, the above steps (1-8) are repeated 13 times, reducing the size of perturbations in step 1 from $\sigma_1 = \frac{1}{4}$ to $\sigma_{13} = \frac{1}{128}$.

A Monte Carlo analysis repeats these steps (Steps 1-9) 1000 times, initiated from a different prior depth-age relationship by randomly perturbing ACPs within their age uncertainty (Table 1). ~~We choose the best realization for gas age constraints for the RICE17 gas age-scale.~~ Parameters used for the synchronization are given in Table 2 for ~~both~~ the 60.06-670.13 m and 670.13-719.30 m intervals~~; 60.05-670.13 m and 670.13-719.30 m~~. Code for the synchronization routine is provided as supplementary material.

We choose the best realization for gas age constraints for the RICE17 gas age-scale. The best age estimate (realization) is not necessarily the most frequent age estimate. Fig. 5d shows an example from sample depth 621.28 m where there is a large difference between these two age estimates. Large differences can occur because the prior age estimate (i.e. the age estimate based only on prior ACPs) differs by a large amount from the "true" age of that sample and because the goodness-of-fit parameter considers the fit over the whole record. For depth 621.28 m most realizations resulted in an age estimate of 9200 yr BP, similar to its prior age estimate of 9,240 yr BP, but the best realization estimated the age to be 9012 yr BP. There are two possible reasons for this type of result: 1) this realization is the best because it managed to push the age of this sample by >200 years towards younger ages while not significantly changing the ages of nearby sections which already fit well, or 2) no significant improvement in the goodness-of-fit was found by adjusting the age of this depth, and the goodness-of-fit was dictated by other sections of the record.

Uncertainty in gas age constraints is calculated as the root-mean-square error of FCP ages from the 1000 Monte Carlo realizations (Fig 4d), although we acknowledge calculating uncertainty as a symmetric Gaussian error that this can overly simplify the empirical distribution of possible ages for a given depth (Fig. 5). Assessing uncertainty in this way integrates two types of error. The first is the ability to exactly match timing of two features. This uncertainty is determined by how well features are resolved in the records, measurement error, and the limited degrees of freedom in synchronization (i.e. the synchronization routine assumes constant accumulation during each subsections in a piece-wise manner, although the true accumulation history is more likely to smoothly vary). The second type of error is analogous to deciding which feature in the reference record is the correct match. For example, the methane peak centered at 459.05 m (4675 yr BP) is, in some realizations, instead matched to a different methane peak observed at ∼4550 yr BP in the WAIS Divide record, providing two distinct age possibilities with some uncertainty about each (Fig. 5c).

4.2 Extending the chronology with visually matched gas age control points: 30-83 ka

Sample The more limited resolution of the RICE methane record below 719.3 m (30.66 ka) prevented use of the automated synchronization routine to synchronize this section of core. Gas age control points were visually chosen between 719.30 m (30.66 ka) and 746.00 m (65.6 ka) and between 746.00 and 752.95 m (∼83 ka) (Table 1). Between 719.30 (30.66 ka) and 746.00 m (65.6 ka), ACPs were visually chosen by comparing the RICE discrete and CFA methane records and the $\delta^{18}O_{atm}$ record to the WAIS Divide methane (Rhodes et al., 2015) and $\delta^{18}O_{atm}$ records (Buizert et al., 2015).

The WAIS Divide records and the WD2014 chronology end at 67.8 ka. For the deeper (older) section of the RICE ice core, between 746.00-752.95 m, we build target records from records of methane and $\delta^{18}O_{atm}$ from the NGRIP ice core (Baumgartner et al., 2014; Landais et al., 2007; **?**). Using the NGRIP ice core is internally consistent with the WD2014 chronology, which is itself tied to a modified GICC05modelext age-scale between 30-67.8 ka (Buizert et al., 2015). Because NGRIP is in the northern hemisphere the methane concentration is higher than that in the RICE record. For the methane target record, we To account for the this interpolar difference we scale the NGRIP target methane record by linearly scaling the record from (Baumgartner et al., 2014) to Antarctic values using an empirical least-squares fit between the NGRIP and WAIS Divide and NGRIP methane records between 55-67.8 ka.

Buizert et al. (2015) found that the annual layer counted portion of the GICC05modelext chronology (0-60 ka) (Andersen et al., 2006; Svensson et al., 2008) is systematically younger than ages of corresponding features found in the U/Th absolute dated Hulu speleothem record (Reimer et al., 2013; Southon et al., 2012). A fit to Hulu ages was optimized by scaling the GICC05modelext ages linearly by 1.0063. This suggests that 6.3 out of every 1000 annual layers were not counted. For our

NGRIP-based target records we adjust the NGRIP age-scale by ~~the target records we~~ adopting the ~~same~~ scaling ~~as~~ of Buizert et al. (2015) ~~for the annual layer counted section of NGRIP, ending at 60 ka in the GICC05modelext chronology and equating to 60.378 ka in WD2014 (and RICE17)~~. Older ages in the ~~Ages older than 60 ka in the~~ GICC05modelext chronology are derived from the ss09sea Dansgaard-Johnsen model (Johnsen et al., 2001; NGRIP Community Members, 2004) ~~which is not susceptible to under counting of annual layers~~. ~~This portion of GICC05modelext was stitched to the annual layer counts by subtracting a constant 705 years (Wolff et al., 2010). For this section of the target NGRIP records,~~ We have added a constant 378 years (0.0063*60,000 yrs) for depths older than ~~is added to the age from GICC05modelext starting at the depth corresponding to~~ 60 ka in the target GICC05modelext ages to make this section continuous with the adjusted annual layer counted section ~~(60.378 ka in WD2014)~~.

Synchronization between records requires ~~the occurrence of identifiable features that are~~ well-sampled identifiable features in both records. We estimate age uncertainty for visually matched ACP's ~~for this set of ACP's~~ (ACP's older than 29.9 ka) as the larger of the sample spacing of the two records being synchronized, following methods of Brook et al. (2005). Gas age uncertainty is plotted in Fig. 4d. The largest uncertainty is ∼1500-1700 years and occurs between 41.7-47.6 ka, ~~when~~ where the age-scale is very compressed and the RICE records are poorly sampled.

4.3 Age control points in the disturbed ice: 746-753 m

Continuity of the RICE ice core appears to end at 746.00 m below surface, where a discontinuity of 20‰ is observed in the ~~RICE~~ δD record (746.00-746.10 m) (Fig. 6b) and a 0.35‰ change is observed between sequential $\delta^{18}O_{atm}$ samples (745.81 and 746.20 m) (Fig. 6c). The continuous chronology described in the previous section dates ~~Methane and $\delta^{18}O_{atm}$ values immediately above this discontinuity date~~ this ice to the end of DO-18 (∼64.6 ka). This age is supported by very negative δD values and a trend to more enriched values at shallower depths which is consistent with warming trends observed in other Antarctic ice cores at this time period (Buizert et al., 2015; EPICA Community Members, 2006; Petit et al., 1999; Parrenin et al., 2013) (Fig. 6f).

Figure 6 presents our best effort to date the ice in the disturbed section, between 746.00 and 752.95 m. The left panel of 6 shows the data as a function of depth, color-coded by age. The right panel shows the reconstructed time history of these variables, color-coded by depth. Below, we discuss how the ages are assigned to different depth sections (divided by vertical red lines in teh left side of 6), starting with the shallowest portion. Dating folded ice remains challenging, and the solution we found may not be unique.

Immediately below the discontinuity, between 746.10-747.85 m, methane and $\delta^{18}O_{atm}$ values best match our target records during DO-20 between 74.5-77.3 ka (Fig. 6), although the RICE methane record appears ∼30 ppb too high. Dating of this section to DO-20 implies that either 9.4 ka of climate history is missing from the RICE ice core because climate was not recorded or that 9.4 ka is compressed into ∼10 cm of ice. Extremely thin layers can be explained by ice flow or by an absence of accumulation, but the latter scenario would cause a collapse of the firn and $\delta^{15}N-N_2$ values approaching 0‰ which are not observed.

A cluster of samples between 747.85-750.46 m are ∼0.16‰ more enriched in $\delta^{18}O_{atm}$ than was observed in the shallower section dated to DO-20 (Fig. 6c). In the NGRIP, EDML, and Siple Dome ice cores, a long term trend in $\delta^{18}O_{atm}$ towards more enriched values is observed from 80 to 65 ka (Capron et al., 2010; Severinghaus et al., 2009; Landais et al., 2007) (Fig. 6g). The enriched values between 748.34-750.46 m most likely indicate that this ice is younger than the adjacent shallower depths and the stratigraphic order is reversed. ~~In t~~This depth range is~~, methane and $\delta^{18}O_{atm}$ values~~ best matched to ~~the atmospheric history of~~ DO-19 between 71.8-74.3 ka (Fig. 6). Below 750.46 m, methane and $\delta^{18}O_{atm}$ return to values that best match DO-20.

~~The depth representing the top of the reversal (the shallowest depth where age begins to get younger at deeper depths) at 747.85 m is marked by a clear minimum in δD (Fig. 6b). The RICE CFA methane data also show a minimum in concentration at this depth, but this record is very erratic during this interval and the coincidence of these two features may not be meaningful. The bottom of the reversal, with the youngest age observed in this section, coincides with another clear minimum in the RICE δD at 749.60 m (Fig. 6b) consistent with a cooling trend which is observed during DO-19 in other Antarctic records (EPICA Community Members, 2006).~~

We note that two significant measurement gaps exist in the ~~RICE~~ δD record, at 746.89-747.07 m and at 750.00-750.25 m (~~red~~ gray bars in Fig. 6b). A 12‰ shift in δD accompanies both of these gaps. The second measurement gap (750.46-750.56 m) is at nearly the same depth which separates the samples dating to DO-19 from the grouping immediately below dated to DO-20. The discontinuity of the δD record at these gaps may signify another hiatus in the climate record or highly contorted layers that are typically found around folds (Cunningham and Waddington, 1990; Alley et al., 1997; Thorsteinsson and Waddington, 2002; Waddington et al., 2001).

Below 750.46 meters, trends in methane and $\delta^{18}O_{atm}$ indicate that the age of ice ~~continues to~~ increases with depth until at least 753 m (∼83 ka). Age of this depth is constrained by a measured $\delta^{18}O_{atm}$ value of -0.175‰. Such a depleted value is rare and only occurs during periods of high sea-level and small ice sheets, the most recent time period prior to the Holocene being MIS-5a (80-85 ka) (Severinghaus et al., 2009; Capron et al., 2010; Petit et al., 1999; Landais et al., 2007). Negative values were observed at two other depths below 753 m (Fig. 2f), but the stratigraphic order of these depths is difficult to assess.

4.4 Dynamic firn model to establish ice age

~~Movement of air within~~ Air transport in the firn causes ~~gases trapped in ice cores to be younger than the ice encapsulating it; this gas age-ice age~~ an age difference between ice and air trapped in the ice, ~~is~~ commonly denoted Δage. Firn densification models are typically used to simulate past Δage (Schwander et al., 1997; Goujon et al., 2003). Input parameters (for example, temperature, accumulation rate, and surface density) are normally the ~~The~~ largest sources of uncertainty ~~error in reconstructing Δage is the input parameters, which are rarely well known~~. Using $\delta^{15}N\text{-}N_2$ as a proxy for past firn column thickness~~,~~ and assuming δD ~~(Bertler, 2018, *personal communication*)~~ records past site temperature faithfully, firn densification models can be run in an inverse mode to estimate both past Δage and accumulation rates (?Buizert et al., 2015) and is the approach we employ here.

~~For the RICE ice core chronology, w~~We use a dynamic version of the Herron-Langway model (Herron and Langway, 1980) which was also used for construction of the WD2014 chronology (Buizert et al., 2015). The model simulates firn compaction rates as well as vertical heat diffusion and advection. The model domain is the full 763 m ice column at 0.5 m resolution; a time step of 1 year is used. The model simulates both gravitational enrichment of δ^{15}N-N_2 and fractionation in the presence of thermal gradients. The model is forced with a temperature history derived from the ~~a record of~~ δD ~~(Bertler, 2018, *personal communication*)~~ record assuming a constant isotope sensitivity of 6‰·K^{-1} (Brook et al., 2005)~~ which, in~~. In conjunction with an assumed geothermal heat flux of 78 mW·m^{-2}, this provides a good fit to the measured borehole temperature profile (Clemens-Sewall et al., Unpublished). This sensitivity ~~for RICE~~ is similar to that observed for West Antarctica (Stenni et al., 2017; Cuffey et al., 2016; Masson-Delmotte et al., 2008) but is somewhat higher than the sensitivity obtained by comparing the RICE isotope record to ERA interim data (Bertler et al., 2018). However, lower sensitivities decreased the fit of the modeled borehole temperature profile. The dependency of ~~our~~ Δage ~~results to~~ on the assumed isotope sensitivity was explored in a model sensitivity test (Appendix C), and ~~are~~ is incorporated into the Δage uncertainty estimates. The model further assumes a constant ice thickness, a constant 2 m convective zone similar to other high accumulation dome sites with low mean wind speeds (Kawamura et al., 2006; **?**), and surface firn density of 400 kg·m^{-3} to match the modern surface firn density.

In a first iteration, we assume a prior ice age-scale for the temperature history by adding a constant 150 years to the gas chronology (Section 4.1 and 4.2). A new Δage solution is then calculated using the dynamic firn densification model. The Δage solution (and thereby the ice age-scale) is refined iteratively until it no longer changes appreciably (consistent within ~1 year).

The climate at Roosevelt Island, with high accumulation and relatively warm temperatures, ~~is conducive to~~ results in small Δage values~~,~~ and consequently~~,~~ relatively low absolute uncertainty in Δage compared to most Antarctic sites. Modern Δage (estimated at 60 m depth, the shallowest measurement of δ^{15}N-N_2) is 146 years with a reconstructed lock-in depth (LID) of 48 m, consistent with the modern density profile (Bertler et al., 2018; Winstrup et al., 2017). ~~The~~ Holocene Δage ~~variations are~~ is small, ~~with Δage values~~ ranging between 140 to 182 years. During the last glacial period~~,~~ simulated Δage values fluctuate between ~150-350 years.

Uncertainties in past Δage include the uncertainty in model inputs ~~of the parameters which constrain the model~~ as well as in the model itself. The uncertainty of the Herron-Langway model is conservatively estimated to be 20% based on differences between firn models (Lundin et al., 2017). We assessed the uncertainty due to model inputs using a steady-state Herron-Langway model that approximates the dynamic version but requires less computational time (Appendix C). In a sensitivity test, we randomly perturb the parameterizations of temperature and LID and assumptions of convective-zone thickness, surface firn density, and geothermal heat flux and recalculate the Δage solution (model parameters and their base values and ranges used in the sensitivity test are provided in Table A1). A total of 6000 iterations were run. The sensitivity tests include a wide range of temperature histories to account for the possibility that some variations in δD were caused by non-thermal effects such as variability in precipitation seasonality, moisture sources adn pathways, and post-depositional vapor exchange. Model sensitivity is reported asthe root-mean-square-error of Δage calculations for each depth. Combined Δage uncertainty, provided in the included age-scale, is the root-sum-squares of the model uncertainty and the model sensitivity.

4.5 Comparison of gas-derived and layer counted chronologies: 0-2,649 yrs BP

The gas-derived ice age-scale provides a chronology from 60 to 753 m depth (Fig. 2) that is independent of ~~and~~ but overlaps the annual layer counted section (0-343.7 m, Winstrup et al. 2017). Figure 7 shows both chronologies ~~derived from annual layer counting and the gas-measurements. D~~ and differences between them ~~two chronologies is shown in Fig. 7b~~ (Positive values indicate that the annual layer counts are older than the gas-derived ages). The gas-derived ice age-scale agrees well with the annual layer counted age-scale, within 33 years, with similar trends in the implied annual layer thickness (Fig. 7c). Differences between chronologies can result from error in the synchronization of gas records, calculation of Δage for either the RICE or WAIS Divide ice cores, interpolation between ACPs, or ~~in counting of~~ annual layer~~s~~ counts in either core ~~the RICE ice core or the WAIS Divide ice core~~ (because the WAIS Divide gas age-scale is modeled from the ice age scale ~~used as a reference for the gas age-scale~~).

The average age difference at depths of FCPs is -1 years (n=18, implied age from gas-derived ice age-scale being older than the layer counted chronology). Root-mean-square of the age difference is 17.3 years. Discrete points in the the gas-derived ice age-scale can also be compared to ~~The gas-derived ice age-scale can also be compared to~~ the age of 67 volcanic peaks identified in the RICE ice core and correlated to peaks identified in the WAIS Divide ice core (open red circles in Fig. 7, Winstrup et al. 2017). Compared to these volcanic peaks, the root-mean-square ice age difference of the gas-derived ice age-scale is 13.6 years from their WD2014 ages. Good agreement between the two approaches gives confidence in the methodology used for the deeper section of the RICE17 chronology. The two largest differences occur at 89.72 m (243 yr BP) and at 169.11 m (757 yr BP) and are +30 years and -33 years, respectively (Fig. 7b). These offsets are similar in magnitude to the individual uncertainties in calculating Δage or in synchronizing the gas records. The small age differences between the two ice chronologies also indicates that our approach to calculating uncertainty is likely conservative.

The RICE17 transitions between the annual layer counted and gas-derived age-scales at 343.7 m, the deepest/oldest FCP for which annual layers were identifiable (Section 4.1). The age difference at this depth is 3 years, with the gas-derived ice age implying an older age than the annual layer counted chronology. This age difference is much less than the respective age uncertainties of 45 years and 111 years (2-σ) for the annual layer counts and gas-derived ice age-scale, respectively. Because of the good agreement between the two ice age-scales, no correction is made for the 3 year offset and the annual layer counted age is used.

5 Results/key observations from the RICE chronology and gas data sets

5.1 ~~New observations of centennial-scale variability in the Holocene methane cycle~~

~~Centennial-scale variability of methane in the late pre-industrial Holocene and Preboreal Holocene has been described from other records (Etheridge et al., 1998; Etheridge et al., 2009; Etheridge et al., 2012; Etheridge et al., 2013; Etheridge et al., 2017). The methane records from the WAIS Divide and RICE ice cores are the highest resolution discrete records of the Holocene and the RICE CFA record is the first continuously measured record of the entire Holocene. Replication of centennial-scale variations in multiple ice cores demonstrates that they are robust features in the atmospheric history. These variations, which are well-defined in the RICE and WAIS Divide records, extend back to the last glacial period, providing new chronostratigraphic targets which can be used to date future ice cores, as we have done for matching the RICE and WAIS Divide ice cores.~~

~~Curiously, over the past 2,000 years, centennial-scale variability of methane only weakly correlates with temperature and precipitation of key methane producing regions (Mitchell et al., 2011), the main climatic factors controlling biogenic methane production (Fung et al., 1991). The apparent lack of coherence with climatic forcing and changes in the stable isotopic composition of methane during this time period has led several studies to propose that this mode of variability may be linked to human population and early-anthropogenic land-use practices (Ferretti et al., 2005; Ferretti et al., 2008; Ferretti et al., 2009; Ferretti et al., 2011; F Anthropogenic forcing is supported by the coincidence of decreasing methane concentration with several well documented declines in global population resulting from disease or war (Mitchell et al., 2011). All of these studies focused on ice core records of methane and the isotopes of methane during the past 2000 years when human population was significant enough to make this idea plausible. The RICE ice core documents that centennial-scale variability of similar magnitude and recurrence is prevalent throughout the last 11.7 ka (Fig. 3), before the rise of agriculture, when estimates of human populations were much lower. Recently, centennial-scale variability has also been documented in much older ice (Rhodes et al., 2017), dating from the last glacial period. This evidence implies that centennial-scale variability can occur solely from natural forcing, but it is not currently clear what that forcing is.~~

5.2 ~~Interpreting the~~ Implied accumulation history of Roosevelt Island ~~from past firn structure~~

From 65 to 32 ka, the low-variability of δ^{15}N-N_2 (ranging from 0.20 to 0.24‰) and the cooling trend observed for Antarctica for this time period suggest a decreasing trend in accumulation. ~~suggests that changes in firn-thickness were also small (Sowers et al., 1989; Sowers et al., 1989) (Fig. 3c). The steady δ^{15}N-N_2 values in combination with the cooling trend observed in Antarctica for this time period suggest a decreasing trend in accumulation (Buizert et al., 2015).~~

While δ^{15}N-N_2 values appear steady from 65 to 32 ka and during the Holocene (Fig. 3c), they exhibit large variability between 32 and 10 ka (Fig. 8a). δ^{15}N-N_2 generally trends to heavier values beginning at 32 ka until 14.71 ka, indicating a growing firn column. An inflection point is observed at 25.3 ka which is interpreted as an acceleration of firn thickening concluding in a peak of 0.293‰ at 21.8 ka. After a short depletion the steep trend resumed with a second δ^{15}N-N_2 maximum of 0.326‰ reached at 15.7 ka. Following this maximum, δ^{15}N-N_2 abruptly decreased from 0.308‰ to 0.220‰ at 14.71 ka, which corresponds with the beginning of the Antarctic Cold Reversal (ACR). At 12.38 ka, after the ACR, δ^{15}N-N_2 partially recovers to pre-ACR values with an abupt increase to 0.260‰.

Between 25.3-32 ka, accumulation ~~was~~ is estimated to be ∼10 cm ice equivalent per year (Fig. 8d) and the increasing firn thickness is largely attributable to decreasing temperature. After 25.3 ka, accumulation starts to increase and by the first δ^{15}N-N_2 maximum (21.8 ka), accumulation had increased to ∼17 cm ice equivalent per year. This feature is not apparent in other ice cores from the Ross Sea region, but those records tend to be difficult to interpret beause of chronological uncertainties, such as is the case for Taylor Dome (Baggenstos et al., 2017), or because of unexplained jumps in δ^{15}N-N_2, such as is the case for Siple Dome (Severinghaus et al., 2009). By the second maximum (15.7 ka) accumulation increased to ∼25 cm ice equivalent per year, similar to accumulation rates observed during the Holocene. An accumulation peak at the end of ~~following~~ glacial terminations is consistent with evidence from trimlines in interior WAIS (Ackert et al., 2013) and is also observed in the accumulation histories from WAIS Divide and Siple Dome (WAIS Divide Project Members, 2013; Waddington et al., 2005), but to a smaller degree. The early accumulation peak at 21.8 ka is unique to the RICE ice core.

A large, rapid depletion in the δ^{15}N-N_2 is observed at 14.71 ka with low values lasting until 12.38 ka. Analysis of the lead-lag relationship between methane and the thermal-signal from δ^{15}N-N_2 has been used to infer a closely coupled climate throughout the tropics and northern hemisphere (**?**). These climate events are believed to originate in the northern hemisphere and propagate to the southern hemisphere (Blunier et al., 1998; Blunier and Brook, 2001; Buizert et al., 2015). Curiously, ~~this~~ the abrupt decrease in δ^{15}N-N_2 at 12.38 ka is observe in samples deeper than the increase in methane ~~precedes the increase in CH_4~~ marking the onset of the Bølling-Allerød meaning that this climate event unambiguously precedes the Northern Hemisphere event. In the firn model, this period of shallow firn thickness is interpreted as ~~caused by~~ a large reduction of snow accumulation (<10 cm/yr, Fig. 8d). Low accumulation during this period is consistent with thin annual layers interpreted from the age-depth relationship (Fig. 3d); 0.3-0.6 cm/yr annual layer thickness compared with 1.6-3.2 cm/yr between 10.09-11.01 ka (642.75-661.07 m). Following the ACR ~~, at 12.38 ka, a rapid increase in accumulation is inferred,~~ the modelled accumulation rate fully recovers~~ing~~ to the ∼25 cm per year observed before the ACR.

We propose three potential explanations for the thin annual layers and low accumulation rate observed during the ACR, with the last explanation being our preferred. 1) A large accumulation gradient is observed across the Roosevelt Island ice dome (Winstrup et al., 2017) which implies that a period of low accumulation may be the result of ~~regional climate changes or changes to the geometry of the Roosevelt Island ice dome~~ migration of the ice divide with respect to the RICE site. However, ~~the long timescales required for~~ ice divide ~~dome~~ migration typically occurs over long timescales ~~may be to slow compared to the abrupt timescale of the inferred accumulation event~~. 2) Accelerated ice flow may cause thin annual layers and could potentially even affect layers within the firn. This flow could be the result of the sudden removal of ~~One mechanism which may cause rapid adjustment of the ice dome location is if~~ the ice streams which surrounded and buttressed Roosevelt Island ~~ice dome were suddenly removed~~ (Ackert et al., 1999, 2013; Halberstadt et al., 2016). ~~In this scenario, the removal of grounded ice around Roosevelt Island would likely have enhanced ice flow within the dome resulting in its thinning and thin annual layers.~~ The timing of the low accumulation interval is similar to when dust records from an ice core from Taylor Dome (Aarons et al., 2016), a site located in the Transantarctic Mountains near the Ross Sea (Fig. 1), imply that the spatial extent of the Ross

Ice Shelf withdrew and is similar to some estimates of the timing of retreat of the WAIS based on sediment facies succession and radiocarbon dating (minimum date of 8.6 ka, McKay et al. 2016) and ~~also~~ ice-sheet modeling ~~(by meltwater pulse-1a, ∼14.7 ka,~~ (Golledge et al., 2014; McKay et al., 2016). Although annual layer thickness immediately above the ACR section is observed to be nearly five times as thick as the ACR section, this large change in thickness, if solely the result of changes in ice flow, would require an unrealistic change in the thickness of the dome or its ice flow which is not supported by TAC measurements or ice-flow modelling.

3) Our ~~Based on physical arguments, our~~ preferred explanation is that an interval of ~~arid conditions~~ low accumulation between 12.38 and 14.71 ka resulted in a shallow firn structure and depleted δ^{15}N-N$_2$ values. In recent times, moisture arriving at Roosevelt Island is frequently related to enhanced cyclonic air flow in the Ross Sea and a strong Amundsen Sea Low (Tuohy et al., 2015; Emanuelsson et al., 2018). This period of low accumulation may indicate a changed atmospheric structure in the South Pacific where southward air flow is blocked by a persistent low pressure zone north of the Ross Sea such as observed in more recent periods in the accumulation record from RICE (Bertler et al., 2018; Emanuelsson et al., 2015) and potentially related to the past ice shelf extent. Such a pronounced minimum in accumulation is not observed in the Siple Dome ice core, where annual layers are observed to thicken during the ACR (Brook et al., 2005; Waddington et al., 2005). If non-thermal effects influenced the RICE δD record, which is interpreted as temperature in our firn model, then the magnitude of accumulation change during this period may not be as large as reconstructed from the firn model. While not currently available, measurements of d$_{excess}$, dust particle size distributions, and dust geochemistry may be helpful in explaining the temperature and accumulation history of RICE.

5.3 Implications for climate and ice sheet history

Early reconstructions of the Ross Ice sheet during the LGM were based on glacial geological constraints from the western margin of the embayment. ~~They showed~~ Denton and Hughes (2002) describe a maximum scenario in which thick ice in the Ross Embayment ~~that~~ overrode both Siple Dome and Roosevelt Island ~~(Denton and Hughes, 2002)~~. However, more recent observations and model experiments indicate a 'fast and thin" sceario in which ~~that~~ Siple Dome was not overrun by the interior ice sheet during the LGM (Waddington et al., 2005; Price et al., 2007) and ~~that although~~ the Ross ice streams likely ~~slowed down during the LGM, they~~ remained active, maintaining a low elevation profile of the ice sheet in the Ross Sea (Parizek and Alley, 2004).

Our results further support this scenario~~,~~ and add~~s~~ a key new constraint on ice thickness and thinning in the Eastern Ross Sea. Specifically, our results suggest that ice deposited on Roosevelt Island originated as accumulation local to the drilling site which may not be true if WAIS was thick during the LGM and overrode Roosevelt Island. If remnants of WAIS were stranded on Roosevelt Island, ~~it may be recognized by~~ this would likely result in a a hiatus in the gas and ice chronology, ~~by~~ in values of δD or TAC characteristic of more continental or much higher elevations, or discontinuities in the δ^{15}N-N$_2$ record indicating a much different firn structure.

While the RICE ice core chronology does exhibit and aburpt shift in δ^{15}N-N$_2$ and TAC during the ACR (Fig. 3), no discontinuity in δD was observed meaning that it is unlikely that any of this ice originated as part of WAIS. At ~~at~~ least one age discontinuity ~~in age~~ (at 64.6 ka) as well as an age reversal was observed deeper in the core, ~~this does~~ these depths do not coincide with the timing of the retreat of WAIS in the Ross Sea (McKay et al., 2016). The largest discontinuity, at 746.00-746.10 m, is accompanied by 20‰ change in δD. ~~a 9.4 ka hiatus. However, the~~ Methane and $\delta^{18}O_{atm}$ indicate that this discontinuity represents a 9.4 ka age gap. Over the same age range (64.6-73 ka) the EDML ice core records a similar ~~observed~~ change in δD (Fig. 6f) indicating that this change in δD is explained by Antarctic climate patterns alone and without invoking large changes in ice sheet configuration. ~~at RICE during this discontinuity is comparable to the change observed in the EDML ice core during the same time period, 65-69 ka and 71-79 ka (Fig. 6f).~~ A possible second discontinuity is observed at 747.00 m depth at a small gap in measurements of 2.7 cm. Ice immediately below 747.00 m is interpreted as being warmer, meaning that this is probably not derived from somewhere upstream in WAIS at a higher elevation (Fig. 6b). Additionally, no dramatic or sudden change in $\delta^{15}N\text{-}N_2$ or TAC was observed in association with either of these discontinuities ~~this depth~~ (Fig. 6). ~~During the ACR, shifts in $\delta^{15}N\text{-}N_2$ and TAC were observed (Fig. 3), however no discontinuities in δD were observed (Bertler, 2018, *personal communication*).~~ We conclude that it is highly unlikely that the accumulation site of the RICE ice core changed during the deglaciation~~. This evidence leads us to believe~~ and that the Roosevelt Island ice dome probably remained independent of an advanced WAIS during the LGM. A similar conclusion was reached about Siple Dome during the LGM (Waddington et al., 2005; Nereson et al., 1998; Price et al., 2007; Parizek and Alley, 2004).

Geomorphological features on the Ross Sea bed do provide evidence of grounded ice north of ~~an expansive ice sheet which extended past~~ Roosevelt Island during the LGM (Shipp et al., 1999; Anderson et al., 1984, 1992, 2014; Halberstadt et al., 2016). ~~The stability of the~~ If these features were formed by an extended WAIS, it would imply that ice ~~Roosevelt Island ice dome and of Siple Dome implies that at this time, WAIS~~ flowed around Roosevelt Island and Siple Dome and therefore was limited in thickness. ~~these sites rather than over them. This observation implies that as WAIS grew spatially, its thickness in the Ross Sea was limited,~~ These conditions ~~that~~ would indicate that ice streams were active throughout the last glacial period. Alternatively, these features may be the result of ice from a different origin. Price et al. (2007) proposed that during the LGM, an ice dome may have existed on Marie Byrd Land. ~~the geomorphological features observed in the eastern Ross Sea may represent building of an ice dome in Marie Byrd Land.~~ The RICE records can not distinguish between these scenarios.

6 Conclusions

We present the RICE17 gas and ice chronologies for the RICE ice core. These timescales date the gas and ice records from the RICE ice core for the last ~83 ka. Between 0-30 ka~~,~~ an automated synchronization routine is used to identify gas age control points that best match the RICE methane and $\delta^{18}O_{atm}$ records to the respective records from the WAIS Divide ice core (WAIS Divide Project Members, 2013; Buizert et al., 2015). This technique requires few prior constraints, accommodates simultaneous synchronization of multiple parameters, and allows assessment of age uncertainty. Unique in this approach is the use of centennial-scale variability of methane for chronostratigraphic matching for ages older than the last ~2,000 years. Synchronization between ice cores for the time period between 30 and 83 ka (719-753 m) was accomplished by manually choosing tie-points. Below 753 m the ice could not be dated with the currently available data. The RICE17 ice age-scale is based on annual layer counts between -62 and 2649 yr BP (0-343.7 m) and for depths below 343.7 m, a separate ice age-scale was derived from the synchronized gas age-scale by adding Δage estimated from a firn model.

A key ~~Key~~ contribution~~s~~ from the development of the RICE17 age scale is ~~include~~ evidence of active ice streams in the Eastern Ross Sea during the last glacial cycle ~~as well observations about pre-anthropogenic variations of methane~~. ~~The former~~ This is supported by the continuous age-scale and continuous records of climate from RICE which imply that the Roosevelt Island ice dome remained stable and independent of WAIS for at least the last 64.6 ka and likely for the last 83 ka. ~~The continuous record of methane from the RICE ice core is the first covering the Holocene. Centennial-scale variability of methane is observed throughout the Holocene and in earlier periods. During the last 2000 years, this mode of variability has been attributed to the influence of early human activity (Ferretti et al., 2005; Ferretti et al., 2008; Ferretti et al., 2009; Ferretti et al., 2011; Ferretti et al., 2013; Fe although the prevalence of these variations prior to significant human populations implies that there may be some other explanation.~~

The RICE ice core provides records of climate, with precise dating, for a scarcely sampled region of Antarctica. Future work will investigate regional climate of the Eastern Ross Sea in comparison to climate records from other sites to better understand spatial patterns around Antarctica, such as during the ACR when Roosevelt Island experienced an interval of particularly low accumulation, and to study the glacial retreat of WAIS in the Ross Sea.

Code and data availability. The following will be made available on public archives: RICE prior age control points, RICE final age control points, RICE17 age-scale interpolated at higher resolution, RICE CH_4, δ^{18}O-O_2, and δ^{15}N-N_2 data, and code for the gas synchronization routine.

Appendix A: Methane Measurements

~~Description of t~~The methodology used at Oregon State University for measuring methane concentration in ice cores was described in Grachev et al. (2009) and Mitchell et al. (2013). ~~To paraphrase~~ Briefly, 40-60 g ice samples are trimmed and placed in glass flasks. The glass flasks are then attached to a high vacuum line and immersed in a chilled ethanol bath set to -63°C to keep the samples frozen. Since Mitchell et al. (2013), insulation has been added around the ethanol bath and above where the flasks are mounted. The added insulation reduced the temperature and water vapor content in the head space of the flasks and decreased their variability ~~decreased the temperature variability of the ethanol bath and of the sample flasks throughout the day allowing for better measurement of pressure and improved signal-to-noise for the chromatograph.~~ Both can affect methane measurements by changing the pressure reading or the retention time of methane in the GC column. We also made efforts to more carefully regulate the amount of ethanol in the chilled bath and temperature of the hot water bath during melting. These steps improved stability of measurements and extraction between days

After laboratory air has been evacuated, the flask~~s~~ valves are closed and the samples are melted in a hot water bath for 30 minutes to liberate air ~~from the sample~~. Samples are ~~then~~ refrozen by immersing the flasks ~~back into~~ in the cold ethanol bath. Once the samples are completely refrozen and the sample flask temperature has stabilized (approximately 1 hour after refreezing begins), methane measurement ~~of the sample for methane concentration~~ is performed by expanding sample air from the flask headspace into a gas chromatograph (GC). Four measurements can be made on each ice sample.

~~A set of c~~Calibration measurements are made on an internal standard which is referenced to several compressed air standards externally calibrated on the NOAA04 scale (**?**). ~~on dry compressed air of known methane concentration (standard gas) by~~ Calibration runs of systematically varying ~~the~~ pressure are made both before adn after samples are measured. ~~of each run. Calibration runs are made both before and after samples are measured.~~ The calibration curve is a least-squares linear regression between pressure and peak area for both sets of calibration runs described by a slope m_{cal} and intercept b_{cal}.

Methane concentration (C) was previously calculated by comparing the sample pressure (P_{meas}) and the peak area (PA_{meas}) from GC analysis to the predicted peak area of the standard gas of equal pressure.

$$C_{raw} = C_{standard} \cdot \frac{PA_{meas} - b_{cal}}{P_{meas} \cdot m_{cal}} \quad \text{(A1)}$$

~~Four measurements can be made on each ice sample.~~ If the two sets of calibration runs are taken individually, interpretation of sample concentrations typically differ by <3 ppb.

In this calculation, the sample pressure is used to quantify the number of moles of air in the sample assuming that the sample temperature remains constant and equal to standard air temperature during calibration runs. However, in a series of dry blank experiments it was determined that sample gas temperature is cooler than the standard gas temperature. We estimate the temperature difference to be 0.42% of the standard air temperature and thus the sample pressure needs to be corrected upwards by that amount. We call this the GC-thermal effect. We now apply the correction to the previous concentration calculation.

$$C_{raw} = C_{standard} \cdot \frac{PA_{meas} - b_{cal}}{P_{meas} \cdot 1.0042 \cdot m_{cal}} \quad \text{(A2)}$$

Results from typical wet blank samples, in which we add standard air over bubble free ice made from Milli-Q ultra-pure water, had shown that these samples are typically 2-3 ppb enriched compared to the standard concentration using the old method for calculating concentration. This agrees with the predicted magnitude of enrichment from the GC-thermal effect of 2.1 ppb.

Several wet blank samples are measured each day and are interspersed between ice core samples. The offset between the measured concentration of the wet blank and the known concentration of the standard gas added is called the “blank” correction. This represents any effects during the sample analysis process which may alter the measured concentration. We bin the wet blank results over the time period for which samples were measured to establish a single blank correction value with an estimated blank correction uncertainty. RICE ice core samples were measured during two separate periods and have separate blank correction values.

Since the OSU analytical methods use a wet extraction technique to liberate ice core air, effects of gas solubility must be accounted for. Methane is more soluble than the major components of air and is preferentially dissolved during the extraction step. This leads to a decrease in the measured concentration compared to the true ice core concentration. Mitchell et al. (2013) empirically derived a solubility correction (S) which we repeated several times for the RICE samples. S is defined as the total amount of methane (gas + dissolved) divided by the amount in gas phase. A solubility value of 1.0165 was used for ice core samples and 1.0079 for bubble free ice.

The "blank" and "solubility" corrections are applied in the following way:

$$C_{corrected} = C_{raw} \cdot S_{sample} - (C_{blank} \cdot S_{blank} - C_{standard}) \tag{A3}$$

This formula differs from that used by Mitchell et al. (2013). In Mitchell et al. (2013) no solubility correction was applied to the bubble free ice samples. The difference results in a constant offset of -7.4 ppb compared to Mitchell et al. (2013).

Appendix B: Calibration of RICE CFA methane

The RICE CFA methane record is qualitatively used for synchronization to the WAIS Divide methane record, and thus careful calibration was not required. Regardless, we present an ad hoc calibration of the RICE CFA methane record based on comparison to the RICE discrete methane record measured at Oregon State University (OSU). The RICE CFA methane record was measured in multiple campaigns and major adjustments ~~and fixes~~ to the analytical system occurred during both of those periods. Calibration of the RICE CFA record is done in a piecewise manner to reflect these changes.

Our calibration scheme accounts for instrument calibration, a concentration-based correction due to instrument sensitivity, and measurement drift, a time-dependent correction. For comparison between datasets, we subsample the CFA data at depths where discrete measurements were made. We first apply the concentration calibration by regressing the sub-sampled CFA methane concentration against the discrete measurement. Drift was accounted for by a second regression comparing the residual of the concentration calibration against either the measurement time or sample depth, which ever provided the better correlation to the discrete dataset. Drift was only a significant factor between 500-680 m depth. Calibration values are given in Table A2.

Uncertainty in the relationship may be caused by measurement uncertainty, which is relatively small, or the uncertainty in the depth registration of the continuous measurements. Uncertainty in the depth registration is relatively unimportant in the top ∼670 m of core. In this section, annual layers are relatively thick and ~~the variability in~~ methane variability is relatively low which results in only minor ~~changes in~~ uncertainty in methane concentration from an error in depth. However, for the deeper section of core, methane concentrations vary rapidly with depth and small errors in the depth registry represents large differences in methane concentration. Because of errors in the depth registry and the sensitivity of the inferred methane concentration, we restrict our calibration scheme to the last ∼39.66 ka (725.63 m) ending after the inclusion of GIS-8.

Appendix C: Steady-State Herron-Langway Sensitivity Test

The gas age-ice age offset (Δage) for the RICE ice core was estimated with a dynamic Herron-Langway model (Buizert et al., 2015). The model is constrained by measurements of δ^{15}N-N_2 (a proxy for firn thickness) and δD (a proxy for past temperature). The dynamic model also assumes a convective zone of 2 m, surface firn density of 400 kg·m^{-3}, and geothermal heat flux of 78 mW·m^{-2}.

A steady-state version of the Herron-Langway model mimics the dynamic version following a similar iterative methodology. A constant Δage estimate is assumed as a prior to assume an ice age scale for the temperature history. The model then calculates a new Δage solution from the temperature and firn thickness histories. This process is repeated until iterations no longer change appreciably.

While the dynamic version is used to establish the Δage history for RICE, the steady state version has the advantage of being computationally faster and is used in a sensitivity test. In this test, we vary prior assumptions about the isotopic temperature sensitivity used to infer past temperature, the convective zone thickness, surface firn density, and assumptions about geothermal induced temperature gradient in the firn. In a Monte Carlo approach, each parameter is given a range of acceptable values from which the steady-state Herron-Langway model calculates the Δage history (Table A1). This is repeated for 6000 realizations. Realizations are rejected if:

- The modelled modern ice age at lock-in depth (LID) is more than 25 years different than the annual layer counted age of that depth (48.57 m, 89 yrs BP).
- The modeled modern accumulation is less than 0.15 or greater than 0.35 m ice per year.
- The isotopic sensitivity is less than 3.2 or greater than 9.6 $‰\cdot K^{-1}$, similar to the range of values observed for West Antarctica (Masson-Delmotte et al., 2008; Cuffey et al., 2016; Stenni et al., 2017). This parameter is randomly chosen from a normal distribution at the beginning of each realization and can fall outside of this range.
- The minimum temperature is less than -60°C.
- The maximum estimated Δage is more than 1000 years.
- Modeled accumulation does not exceed 1.0 m ice per year and is never negative.

Δage is calculated for each depth that $\delta^{15}N-N_2$ was measured. Uncertainty in Δage is assumed to be the root-mean-square-error of accepted realizations and is estimated for each sample depth.

Author contributions. JEL measured CH_4 at OSU on RICE samples. JEL, NANB, T. Baisden, T. Blunier, VGC, EDK, and PV participated in the 2013 or 2014 continuous flow analysis campaigns. JPS measured $\delta^{15}N-N_2$ and $\delta^{18}O-O_2$ at SIO. JEL, CB, TJF, MW, EB, DDJ, FP, JPS, and EDW contributed to methods and discussion leading to the development of the RICE17 age scale. JEL, HC, TJF, RH, JPS, and EDW contributed with discussion of glaciological interpretations of the ice core record. All authors provided valuable feedback and made helpful contributions to writing the manuscript.

Competing interests. The authors declare no conflicts of interest.

Acknowledgements. This work is a contribution to the Roosevelt Island Climate Evolution (RICE) Program, with contributions from USA, UK, Sweden, New Zealand, Italy, Germany, Australia, China Denmark, Germany, Italy, China, Denmark, and Australia. The US contribution was funded by grants from the US National Science Foundation Office of Polar Sciences (0944021, 0837883, 0944307, 1042883 & 1643394). The NZ contribution was funded through New Zealand Ministry of Business, Innovation, and Employment grants issued through Victoria University (RDF-VUW-1103, 15-VUW-131), GNS Science (540GCT32, 540GCT12) and Antarctica New Zealand (K049). The Danish contribution was funded by the Carlsberg Foundation's North-South Climate Connections project grant. The research also received funding from the European Research Council under the European Community's Seventh Framework Programme (FP7/2007-2013) ERC grant agreement 610055 as part of the Ice2Ice project.

We thank Micheal Rebarchik and Will Patterson for laboratory assistance at Oregon State University. We thank Ross Beaudette for laboratory assistance at Scripps Institution of Oceanography. We thank Marius Simonsen, Helle Kjær, Rebecca Pyne, Daniel Emanuelsson, Bernadette Proemse, Ross Edwards, Darcy Mandeno, and the rest of the RICE team for participation in preparing ice samples and operating instruments during the continuous melting campaigns at GNS. We thank the US Antarctic Support Contractor, Antarctica NZ, the US Air Force, the Air National Guard, and Kenn Borek Air for logistical and field support.

References

Aarons, S., Aciego, S., Gabrielli, P., Delmonte, B., Koornneef, J., Wegner, A., and Blakowski, M.: The impact of glacier retreat from the Ross Sea on local climate: Characterization of mineral dust in the Taylor Dome ice core, East Antarctica, Earth and Planetary Science Letters, 444, 34–44, https://doi.org/10.1016/j.epsl.2016.03.035, 2016.

Ackert, R. P., Barclay, D. J., Borns, H. W., Calkin, P. E., Kurz, M. D., Fastook, J. L., and Steig, E. J.: Measurements of Past Ice Sheet Elevations in Interior West Antarctica, Science, 286, 276–280, https://doi.org/10.1126/science.286.5438.276, https://doi.org/10.1126/science.286.5438.276, 1999.

Ackert, R. P., Mukhopadhyay, S., Parizek, B. R., and Borns, H. W.: Ice elevation near the West Antarctic Ice Sheet divide during the last glaciation, Geophysical Research Letters, 34, https://doi.org/10.1029/2007GL031412, 2007.

Ackert, R. P., Putnam, A. E., Mukhopadhyay, S., Pollard, D., DeConto, R. M., Kurz, M. D., and Borns, H. W.: Controls on interior West Antarctic Ice Sheet Elevations: inferences from geologic constraints and ice sheet modeling, Quaternary Science Reviews, 65, 26–38, https://doi.org/10.7916/D8CG010P, 2013.

Alley, R. B., Shuman, C. A., Meese, D. A., Gow, A. J., Taylor, K. C., Cuffey, K. M., Fitzpatrick, J. J., Grootes, P. M., Zielinski, G. A., Ram, M., Spinelli, G., and Elder, B.: Visual-stratigraphic dating of the GISP2 ice core: Basis, reproducibility, and application, Journal of Geophysical Research: Oceans, 102, 26 367–26 381, https://doi.org/10.1029/96jc03837, http://dx.doi.org/10.1029/96JC03837, 1997.

Andersen, K. K., Svensson, A., Johnsen, S. J., Rasmussen, S. O., Bigler, M., Röthlisberger, R., Ruth, U., Siggaard-Andersen, M.-L., Steffensen, J. P., Dahl-Jensen, D., Vinther, B. M., and Clausen, H. B.: The Greenland Ice Core Chronology 2005, 15-42 ka. Part 1: constructing the time scale, Quaternary Science Reviews, 25, 3246–3257, https://doi.org/10.1016/j.quascirev.2006.08.002, 2006.

Anderson, J. B., Brake, C. F., and Myers, N. C.: Sedimentation on the Ross Sea continental shelf, Antarctica, Marine Geology, 57, 295–333, https://doi.org/10.1016/0025-3227(84)90203-2, 1984.

Anderson, J. B., Shipp, S. S., Bartek, L. R., and Reid, D. E.: Evidence for a grounded ice sheet on the Ross Sea continental shelf during the late Pleistocene and preliminary paleodrainage reconstruction, Contributions to Antarctic Research III, pp. 39–62, https://doi.org/10.1029/AR057p0039, 1992.

Anderson, J. B., Conway, H., Bart, P. J., Witus, A. E., Greenwood, S. L., McKay, R. M., Hall, B. L., Ackert, R. P., Licht, K., Jakobsson, M., et al.: Ross Sea paleo-ice sheet drainage and deglacial history during and since the LGM, Quaternary Science Reviews, 100, 31–54, https://doi.org/10.1016/j.quascirev.2013.08.020, 2014.

Aydin, M., Montzka, S. A., Battle, M. O., Williams, M. B., De Bruyn, W. J., Butler, J. H., Verhulst, K. R., Tatum, C., Gun, B. K., Plotkin, D. A., Hall, B. D., and Saltzman, E. S.: Post-coring entrapment of modern air in some shallow ice cores collected near the firn-ice transition: evidence from CFC-12 measurements in Antarctic firn air and ice cores, Atmospheric Chemistry and Physics, 10, 5135–5144, https://doi.org/10.5194/acp-10-5135-2010, https://doi.org/10.5194/acp-10-5135-2010, 2010.

Baggenstos, D., Bauska, T. K., Severinghaus, J. P., Lee, J. E., Schaefer, H., Buizert, C., Brook, E. J., Shackleton, S., and Petrenko, V. V.: Atmospheric gas records from Taylor Glacier, Antarctica, reveal ancient ice with ages spanning the entire last glacial cycle, Climate of the Past, 13, 943–958, https://doi.org/10.5194/cp-13-943-2017, https://www.clim-past.net/13/943/2017/, 2017.

Baumgartner, M., Kindler, P., Eicher, O., Floch, G., Schilt, A., Schwander, J., Spahni, R., Capron, E., Chappellaz, J., Leuenberger, M., Fischer, H., and Stocker, T. F.: NGRIP CH_4 concentration from 120 to 10 kyr before present and its relation to a δ^{15}N temperature reconstruction from the same ice core, Climate of the Past, 10, 903–920, https://doi.org/10.5194/cp-10-903-2014, https://doi.org/10.5194/cp-10-903-2014, 2014.

Bender, M., Labeyrie, L., Raynaud, D., and Lorius, C.: Isotopic composition of atmospheric O_2 in ice linked with deglaciation and global primary productivity, Nature, 318, 349–353, https://doi.org/10.1038/318349a0, 1985.

Bender, M. L., Sowers, T., Barnola, J., and Chappellaz, J.: Changes in the O_2/N_2 ratio of the atmosphere during recent decades reflected in the composition of air in the firn at Vostok Station, Antarctica, Geophysical Research Letters, 21, 189–192, https://doi.org/10.1029/93gl03548, http://dx.doi.org/10.1029/93GL03548, 1994.

Bentley, M. J., Cofaigh, C. Ó., Anderson, J. B., Conway, H., Davies, B., Graham, A. G., Hillenbrand, C.-D., Hodgson, D. A., Jamieson, S. S., Larter, R. D., et al.: A community-based geological reconstruction of Antarctic Ice Sheet deglaciation since the Last Glacial Maximum, Quaternary Science Reviews, 100, 1–9, https://doi.org/10.1016/j.quascirev.2014.06.025, 2014.

Bertler, N.: RICE δD-H_2O record, personal communication, data embargoed at time of submission., 2018, *personal communication*.

Bertler, N. A., Conway, H., Dahl-Jensen, D., Emanuelsson, D. B., Winstrup, M., Vallelonga, P. T., Lee, J. E., Brook, E. J., Severinghaus, J. P., Fudge, T. J., et al.: The Ross Sea Dipole-temperature, snow accumulation and sea ice variability in the Ross Sea region, Antarctica, over the past 2700 years, Climate of the Past, 14, 193, https://doi.org/10.5194/cp-14-193-2018, 2018.

Blunier, T. and Brook, E. J.: Timing of millennial-scale climate change in Antarctica and Greenland during the last glacial period, Science, 291, 109–112, https://doi.org/10.1126/science.291.5501.109, 2001.

Blunier, T., Chappellaz, J., Schwander, J., Dällenbach, A., Stauffer, B., Stocker, T. F., Raynaud, D., Jouzel, J., Clausen, H. B., Hammer, C. U., and Johnsen, S. J.: Asynchrony of Antarctic and Greenland climate change during the last glacial period, Nature, 394, 739–743, https://doi.org/10.1038/29447, http://dx.doi.org/10.1038/29447, 1998.

Brook, E. J., White, J. W. C., Schilla, A. S. M., Bender, M. L., Barnett, B., Severinghaus, J. P., Taylor, K. C., Alley, R. B., and Steig, E. J.: Timing of millennial-scale climate change at Siple Dome, West Antarctica, during the last glacial period, Quaternary Science Reviews, 24, 1333–1343, https://doi.org/10.1016/j.quascirev.2005.02.002, https://doi.org/10.1016/j.quascirev.2005.02.002, 2005.

Buizert, C., Cuffey, K. M., Severinghaus, J. P., Baggenstos, D., Fudge, T. J., Steig, E. J., Markle, B. R., Winstrup, M., Rhodes, R. H., Brook, E. J., Sowers, T. A., Clow, G. D., Cheng, H., Edwards, L. R., Sigl, M., McConnell, J. R., and Taylor, K. C.: The WAIS Divide deep ice core WD2014 chronology – part 1: Methane synchronization (68-31 ka BP) and the gas age-ice age difference, Climate of the Past, 11, 153–173, https://doi.org/10.5194/cp-11-153-2015, https://doi.org/10.5194/cp-11-153-2015, 2015.

Buizert, C., Adrian, B., Ahn, J., Albert, M., Alley, R. B., Baggenstos, D., Bauska, T. K., Bay, R. C., Bencivengo, B. B., Bentley, C. R., Brook, E. J., Chellman, N. J., Clow, G. D., Cole-Dai, J., Conway, H., Cravens, E., Cuffey, K. M., Dunbar, N. W., Edwards, J. S., Fegyveresi, J. M., Ferris, D. G., Fitzpatrick, J. J., Fudge, T. J., Gibson, C. J., Gkinis, V., Goet, J. J., Gregory, S., Hargreaves, G. M., Iverson, N., Johnson, J. A., Jones, T. R., Kalk, M. L., Kippenhan, M. J., Koffman, B. G., Kreutz, K., Kuhl, T. W., Lebar, D. A., Lee, J. E., Marcott, S. A., Markle, B. M., Maselli, O. J., McConnell, J. R., McGwire, K. C., Mitchell, L. E., Mortensen, N. B., Neff, P. D., Nishiizumi, K., Nunn, R. M., Orsi, A. J., Pasteris, D. R., Pedro, J. B., Pettit, E. C., Price, P. B., Priscu, J. C., Rhodes, R. H., Rosen, J. L., Schauer, A. J., Schoenemann, S. W., Sendelbach, P. J., Severinghaus, J. P., Shturmakov, A. J., Sigl, M., Slawny, K. R., Souney, J. M., Sowers, T. A., Spencer, M. K., Steig, E. J., Taylor, K. C., Twickler, M. S., Vaughn, B. H., Voigt, D. E., Waddington, E. D., Welten, K. C., Wendricks, A. W., White, J. W. C., Winstrup, M., Wong, G. J., and Woodruff, T. E.: Precise interpolar phasing of abrupt climate change during the last ice age, Nature, 520, 661, 2015a.

Capron, E., Landais, A., Chappellaz, J., Schilt, A., Buiron, D., Dahl-Jensen, D., Johnsen, S. J., Jouzel, J., Lemieux-Dudon, B., Loulergue, L., Leuenberger, M., Masson-Delmotte, V., Meyer, H., Oerter, H., and Stenni, B.: Millennial and sub-millennial scale climatic variations recorded in polar ice cores over the last glacial period, Climate of the Past, 6, 345–365, https://doi.org/10.5194/cp-6-345-2010, https://doi.org/10.5194/cp-6-345-2010, 2010.

Church, J. A., Clark, P. U., Cazenave, A., Gregory, J. M., Jevrejeva, S., Levermann, A., Merrifield, M. A., Milne, G. A., Nerem, R. S., Nunn, P. D., et al.: Sea-level rise by 2100, Science, 342, 1445–1445, https://doi.org/10.1126/science.342.6165.1445-a, 2013.

Clark, P. U. and Tarasov, L.: Closing the sea level budget at the Last Glacial Maximum, Proceedings of the National Academy of Sciences, 111, 15 861–15 862, https://doi.org/10.1073/pnas.1418970111, 2014.

Clemens-Sewall, D., Hawley, R., Conway, H., Brook, E., and Bertler, N.: Paleoclimate of the Ross Sea Region, from Roosevelt Island Borehole Thermometry, Unpublished.

Conway, H., Hall, B., Denton, G., Gades, A., and Waddington, E.: Past and future grounding-line retreat of the West Antarctic Ice Sheet, Science, 286, 280–283, https://doi.org/10.1126/science.286.5438.280, 1999.

Cuffey, K. M., Clow, G. D., Steig, E. J., Buizert, C., Fudge, T., Koutnik, M., Waddington, E. D., Alley, R. B., and Severinghaus, J. P.: Deglacial temperature history of West Antarctica, Proceedings of the National Academy of Sciences, 113, 14 249–14 254, https://doi.org/10.1073/pnas.1609132113, 2016.

Cunningham, J. and Waddington, E.: Boudinage: a source of stratigraphic disturbance in glacial ice in central Greenland, Journal of Glaciology, 36, 269–272, 1990.

David, T. W. E., Priestley, R. E., and Shackleton, E. H.: British Antarctic Expedition, 1907-9, under the command of Sir E.H. Shackleton, c.v.o. Reports on the scientific investigations., vol. v. 1-2 Biology (1910-11), London,W. Heinemann,, http://www.biodiversitylibrary.org/item/62967, http://www.biodiversitylibrary.org/bibliography/22427 — Biology, edited by James Murray. — Geology, edited by T.W.E. David and R.E. Priestley. — The two volumes on biology were issued in parts, those of each volume paged continuously, and are without title-pages. — "No further publications in this series are contemplated."–Publisher's announcement in Geology, v. 2, 1916. — [Ser. 1] Biology: vol. I. I. On collecting at Cape Royds, by J. Murray. 1910. II. On microscopic life in Cape Royds, by J. Murray. 1910. III. Antarctic Rotifera, by J. Murray. 1910. IV. Musci, by J. C, 1910-11.

Debenham, F.: British Antarctic ("Terra Nova") Expedition, 1910, Natural History Report: Recent and Local Deposits of McMurdo Sound Region, vol. Geology vol. 1, London,W. Heinemann, https://hdl.handle.net/2027/osu.32435013905740, 1921.

DeConto, R. M. and Pollard, D.: Contribution of Antarctica to past and future sea-level rise, Nature, 531, 591–597, https://doi.org/10.1038/nature17145, 2016.

Denton, G. H. and Hughes, T. J.: Reconstructing the Antarctic Ice Sheet at the Last Glacial Maximum, Quaternary Science Reviews, 21, 193–202, https://doi.org/10.1016/S0277-3791(01)00090-7, https://doi.org/10.1016/S0277-3791(01)00090-7, 2002.

Denton, G. H. and Marchant, D. R.: The geologic basis for a reconstruction of a grounded ice sheet in McMurdo Sound, Antarctica, at the last glacial maximum, Geografiska Annaler: Series A, Physical Geography, 82, 167–211, https://doi.org/10.1111/j.0435-3676.2000.00121.x, 2000.

Denton, G. H., Bockheim, J. G., Wilson, S. C., and Stuiver, M.: Late Wisconsin and early Holocene glacial history, inner Ross embayment, Antarctica, Quaternary Research, 31, 151–182, https://doi.org/10.1016/0033-5894(89)90004-5, 1989.

Edwards, J., Brook, E., Buizert, C., Sowers, T., Alley, R. Severinghaus, J., Fegyversi, J., Mitchell, L., Grachev, A., Ahn, J., Lee, J., and Rebarchik, M.: High-resolution total air content from the GISP2 Ice Core: New insights into processes controlling pore volume during the firn ice transition, this manuscript contains descriptions of the methodology for the measurement and calculation of TAC as well as a compilation of datasets from samples previously measured at Oregon State University., in prep.

Emanuelsson, B., Baisden, W., Bertler, N., Keller, E., and Gkinis, V.: High-resolution continuous flow analysis setup for water isotopic measurement from ice cores using laser spectroscopy, Atmospheric Measurement Techniques, 8, 2869–2883, https://doi.org/10.5194/amtd-7-12081-2014, 2015.

Emanuelsson, B. D., Bertler, N. A., Neff, P. D., Renwick, J. A., Markle, B. R., Baisden, W. T., and Keller, E. D.: The role of Amundsen–Bellingshausen Sea anticyclonic circulation in forcing marine air intrusions into West Antarctica, Climate Dynamics, pp. 1–18, https://doi.org/10.1007/s00382-018-4097-3, 2018.

EPICA Community Members: One-to-one coupling of glacial climate variability in Greenland and Antarctica, Nature, 444, 195–198, https://doi.org/10.1038/nature05301, https://doi.org/10.1038/nature05301, 2006.

Etheridge, D. M., Steele, L. P., Francey, R. J., and Langenfelds, R. L.: Atmospheric methane between 1000 A.D. and present: Evidence of anthropogenic emissions and climatic variability, Journal of Geophysical Research, 103, 15 979–15 993, https://doi.org/10.1029/98jd00923, http://dx.doi.org/10.1029/98JD00923, 1998.

Feldmann, J. and Levermann, A.: Collapse of the West Antarctic Ice Sheet after local destabilization of the Amundsen Basin, Proceedings of the National Academy of Sciences, 112, 14 191–14 196, https://doi.org/10.1073/pnas.1512482112, 2015.

Ferretti, D. F., Miller, J. B., White, J. W. C., Etheridge, D. M., Lassey, K. R., Lowe, D. C., Meure, C. M. M., Dreier, M. F., Trudinger, C. M., van Ommen, T. D., and Langenfelds, R. L.: Unexpected changes to the global methane budget over the past 2000 years, Science, 309, 1714–1717, https://doi.org/10.1126/science.1115193, https://doi.org/10.1126/science.1115193, 2005.

Fretwell, P., Pritchard, H. D., Vaughan, D. G., Bamber, J. L., Barrand, N. E., Bell, R., Bianchi, C., Bingham, R. G., Blankenship, D. D., Casassa, G., Catania, G., Callens, D., Conway, H., Cook, A. J., Corr, H. F. J., Damaske, D., Damm, V., Ferraccioli, F., Forsberg, R., Fujita, S., Gim, Y., Gogineni, P., Griggs, J. A., Hindmarsh, R. C. A., Holmlund, P., Holt, J. W., Jacobel, R. W., Jenkins, A., Jokat, W., Jordan, T., King, E. C., Kohler, J., Krabill, W., Riger-Kusk, M., Langley, K. A., Leitchenkov, G., Leuschen, C., Luyendyk, B. P., Matsuoka, K., Mouginot, J., Nitsche, F. O., Nogi, Y., Nost, O. A., Popov, S. V., Rignot, E., Rippin, D. M., Rivera, A., Roberts, J., Ross, N., Siegert, M. J., Smith, A. M., Steinhage, D., Studinger, M., Sun, B., Tinto, B. K., Welch, B. C., Wilson, D., Young, D. A., Xiangbin, C., and Zirizzotti, A.: Bedmap2: improved ice bed, surface and thickness datasets for Antarctica, The Cryosphere, 7, https://doi.org/10.5194/tc-7-375-2013, https://doi.org/10.5194/tc-7-375-2013, 2013.

Fung, I., John, J., Lerner, J., Matthews, E., Prather, M., Steele, L., and Fraser, P.: Three-dimensional model synthesis of the global methane cycle, Journal of Geophysical Research: Atmospheres, 96, 13 033–13 065, https://doi.org/10.1029/91JD01247, 1991.

Golledge, N., Menviel, L., Carter, L., Fogwill, C., England, M., Cortese, G., and Levy, R.: Antarctic contribution to meltwater pulse 1A from reduced Southern Ocean overturning, Nature Communications, 5, 5107, https://doi.org/10.1038/ncomms6107, 2014.

Goujon, C., Barnola, J. M., and Ritz, C.: Modeling the densification of polar firn including heat diffusion: Application to close-off characteristics and gas isotopic fractionation for Antarctica and Greenland sites, Journal of Geophysical Research: Atmospheres, 108, 18, https://doi.org/10.1029/2002jd003319, https://doi.org/10.1029/2002JD003319, 2003.

Grachev, A. M., Brook, E. J., Severinghaus, J. P., and Pisias, N. G.: Relative timing and variability of atmospheric methane and GISP2 oxygen isotopes between 68 and 86 ka, Global Biogeochemical Cycles, 23, 2009, https://doi.org/10.1029/2008GB003330, 2009.

Halberstadt, A. R. W., Simkins, L. M., Greenwood, S. L., and Anderson, J. B.: Past ice-sheet behaviour: retreat scenarios and changing controls in the Ross Sea, Antarctica, The Cryosphere, 10, 1003–1020, https://doi.org/10.5194/tc-10-1003-2016, https://doi.org/10.5194/tc-10-1003-2016, 2016.

Hattori, A.: Denitrification and dissimilatory nitrate reduction, pp. 191–232, Academic Press New York, 1983.

Herron, M. M. and Langway, C. C.: Firn densification: An empirical model, Journal Glaciology, 25, 373–385, https://doi.org/10.3189/S0022143000015239, 1980.

Horibe, Y., Shigehara, K., and Langway, C. C.: Chemical and isotopic composition of air inclusions in a Greenland ice core, Earth and Planetary Science Letters, 73, 207–210, https://doi.org/10.1016/0012-821X(85)90069-X, 1985.

Houweling, S., Van der Werf, G., Klein Goldewijk, K., Röckmann, T., and Aben, I.: Early anthropogenic CH_4 emissions and the variation of CH_4 and $^{13}CH_4$ over the last millennium, Global Biogeochemical Cycles, 22, https://doi.org/10.1029/2007GB002961, 2008.

Hughes, T.: Is the West Antarctic ice sheet disintegrating?, Journal of Geophysical Research, 78, 7884–7910, https://doi.org/10.1029/JC078i033p07884, 1973.

Huybers, P. and Wunsch, C.: A depth-derived Pleistocene age model: Uncertainty estimates, sedimentation variability, and nonlinear climate change, Paleoceanography, 19, https://doi.org/10.1029/2002PA000857, 2004.

Jevrejeva, S., Grinsted, A., and Moore, J. C.: Upper limit for sea level projections by 2100, Environmental Research Letters, 9, 104 008, https://doi.org/10.1088/1748-9326/9/10/104008, 2014.

Johnsen, S. J., Dahl-Jensen, D., Gundestrup, N., Steffensen, J. P., Clausen, H. B., Miller, H., Masson-Delmotte, V., Sveinbjörnsdottir, A. E., and White, J.: Oxygen isotope and palaeotemperature records from six Greenland ice-core stations: Camp Century, Dye-3, GRIP, GISP2, Renland and NorthGRIP, Journal of Quaternary Science, 16, 299–307, https://doi.org/10.1002/jqs.622, http://dx.doi.org/10.1002/jqs.622, 2001.

Kawamura, K., Severinghaus, J. P., Ishidoya, S., Sugawara, S., Hashida, G., Motoyama, H., Fujii, Y., Aoki, S., and Nakazawa, T.: Convective mixing of air in firn at four polar sites, Earth and Planetary Science Letters, 244, 672–682, http://dx.doi.org/10.1016/j.epsl.2006.02.017, 2006.

Kindler, P., Guillevic, M., Baumgartner, M., Schwander, J., Landais, A., and Leuenberger, M.: Temperature reconstruction from 10 to 120 kyr b2k from the NGRIP ice core, Climate of the Past, 10, 887–902, https://doi.org/10.5194/cp-10-887-2014, https://doi.org/10.5194/cp-10-887-2014, 2014.

Kingslake, J., Hindmarsh, R. C., Aðalgeirsdóttir, G., Conway, H., Corr, H. F., Gillet-Chaulet, F., Martín, C., King, E. C., Mulvaney, R., and Pritchard, H. D.: Full-depth englacial vertical ice sheet velocities measured using phase-sensitive radar, Journal of Geophysical Research: Earth Surface, 119, 2604–2618, https://doi.org/10.1002/2014JF003275, 2014.

Landais, A., Masson-Delmotte, V., Combourieu Nebout, N., Jouzel, J., Blunier, T., Leuenberger, M., Dahl-Jensen, D., and Johnsen, S.: Millenial scale variations of the isotopic composition of atmospheric oxygen over Marine Isotopic Stage 4, Earth and Planetary Science Letters, 258, 101–113, https://doi.org/10.1016/j.epsl.2007.03.027, https://doi.org/10.1016/j.epsl.2007.03.027, 2007.

Lundin, J. M., Stevens, C. M., Arthern, R., Buizert, C., Orsi, A., Ligtenberg, S. R., Simonsen, S. B., Cummings, E., Essery, R., Leahy, W., et al.: Firn Model Intercomparison Experiment (FirnMICE), Journal of Glaciology, 63, 401–422, https://doi.org/10.1017/jog.2016.114, 2017.

Martín, C., Hindmarsh, R. C., and Navarro, F. J.: Dating ice flow change near the flow divide at Roosevelt Island, Antarctica, by using a thermomechanical model to predict radar stratigraphy, Journal of Geophysical Research: Earth Surface (2003–2012), 111, 2006.

Martinerie, P., Lipenkov, V. Y., and Raynaud, D.: Correction of air-content measurements in polar ice for the effect of cut bubbles at the surface of the sample, Journal of Glaciology, 36, 299–303, https://doi.org/10.3189/002214390793701282, 1990.

Martinerie, P., Raynaud, D., Etheridge, D. M., Barnola, J. M., and Mazaudier, D.: Physical and climatic parameters which influence the air content in polar ice, Earth Planetary Science Letters, 112, 1–13, https://doi.org/10.1016/0012-821X(92)90002-D, 1992.

Masson-Delmotte, V., Hou, S., Ekaykin, A., Jouzel, J., Aristarain, A., Bernardo, R., Bromwich, D., Cattani, O., Delmotte, M., Falourd, S., et al.: A review of Antarctic surface snow isotopic composition: Observations, atmospheric circulation, and isotopic modeling, Journal of Climate, 21, 3359–3387, https://doi.org/10.1175/2007JCLI2139.1, 2008.

McKay, R., Golledge, N. R., Maas, S., Naish, T., Levy, R., Dunbar, G., and Kuhn, G.: Antarctic marine ice-sheet retreat in the Ross Sea during the early Holocene, Geology, 44, 7–10, https://doi.org/10.1130/G37315.1, 2016.

Mischler, J. A., Sowers, T. A., Alley, R. B., Battle, M., McConnell, J. R., Mitchell, L., Popp, T., Sofen, E., and Spencer, M. K.: Carbon and hydrogen isotopic composition of methane over the last 1000 years, Global Biogeochemical Cycles, 23, https://doi.org/10.1029/2009gb003460, http://dx.doi.org/10.1029/2009GB003460, 2009.

Mitchell, L., Brook, E., Lee, J. E., Buizert, C., and Sowers, T.: Constraints on the Late Holocene Anthropogenic Contribution to the Atmospheric Methane Budget, Science, 342, 964–966, https://doi.org/10.1126/science.1238920, https://doi.org/10.1126/science.1238920, 2013.

Mitchell, L. E., Brook, E. J., Sowers, T., McConnell, J. R., and Taylor, K.: Multidecadal variability of atmospheric methane, 1000-1800 C.E, Journal of Geophysical Research, 116, G02 007, https://doi.org/10.1029/2010jg001441, http://dx.doi.org/10.1029/2010JG001441, 2011.

Mitchell, L. E., Buizert, C., Brook, E. J., Breton, D. J., Fegyveresi, J., Baggenstos, D., Orsi, A., Severinghaus, J., Alley, R. B., Albert, M., Rhodes, R. H., McConnell, J. R., Sigl, M., Maselli, O., Gregory, S., and Ahn, J.: Observing and modeling the influence of layering on bubble trapping in polar firn, Journal of Geophysical Research: Atmospheres, 120, 2558–2574, https://doi.org/10.1002/2014JD022766, https://doi.org/10.1002/2014JD022766, 2015.

Nereson, N., Raymond, C., Waddington, E., and Jacobel, E.: Migration of the Siple Dome ice divide, West Antarctica, Journal of Glaciology, 44, 643–652, https://doi.org/10.3189/S0022143000002148, https://doi.org/10.3189/S0022143000002148, 1998.

NGRIP Community Members: High-resolution record of Northern Hemisphere climate extending into the last interglacial period, Nature, 431, 147–151, https://doi.org/10.1038/nature02805, ://000223746000034, 2004.

Nye, J.: Correction factor for accumulation measured by the thickness of the annual layers in an ice sheet, Journal of Glaciology, 4, 785–788, https://doi.org/10.3189/S0022143000028367, 1963.

Parizek, B. R. and Alley, R. B.: Ice thickness and isostatic imbalances in the Ross Embayment, West Antarctica: model results, Global and Planetary Change, 42, 265–278, https://doi.org/10.1016/j.gloplacha.2003.09.005, 2004.

Parrenin, F., Masson-Delmotte, V., Köhler, P., Raynaud, D., Paillard, D., Schwander, J., Barbante, C., Landais, A., Wegner, A., and Jouzel, J.: Synchronous change of atmospheric CO_2 and Antarctic temperature during the last deglacial warming, Science, 339, 1060–1063, https://doi.org/10.1126/science.1226368, https://doi.org/10.1126/science.1226368, 2013.

Petit, J. R., Jouzel, J., Raynaud, D., Barkov, N. I., Barnola, J. M., Basile, I., Bender, M., Chappellaz, J., Davis, M., Delaygue, G., Delmotte, M., Kotlyakov, V. M., Legrand, M., Lipenkov, V. Y., Lorius, C., Pepin, L., Ritz, C., Saltzman, E., and Stievenard, M.: Climate and atmospheric history of the past 420,000 years from the Vostok ice core, Antarctica, Nature, 399, 429–436, https://doi.org/10.1038/20859, 1999.

Petrenko, V. V., Severinghaus, J. P., Brook, E. J., Reeh, N., and Schaefer, H.: Gas records from the West Greenland ice margin covering the Last Glacial Termination: a horizontal ice core, Quaternary Science Reviews, 25, 865–875, https://doi.org/10.1016/j.quascirev.2005.09.005, 2006.

Pollard, D., DeConto, R. M., and Alley, R. B.: Potential Antarctic Ice Sheet retreat driven by hydrofracturing and ice cliff failure, Earth and Planetary Science Letters, 412, 112–121, https://doi.org/10.1016/j.epsl.2014.12.035, 2015.

Price, S., Conway, H., and Waddington, E.: Evidence for late Pleistocene thinning of Siple Dome, West Antarctica, Journal of Geophysical Research: Earth Surface, 112, https://doi.org/10.1029/2006JF000725, https://doi.org/10.1029/2006JF000725, 2007.

Pyne, R. L., Keller, E. D., Canessa, S., Bertler, N. A., Pyne, A. R., Mandeno, D., Vallelonga, P., Semper, S., Kjær, H. A., Hutchinson, E., and Baisden, W. T.: A novel approach to process brittle ice for continuous flow analysis of stable water isotopes, Journal of Glaciology, 64, 289–299, https://doi.org/10.1017/jog.2018.19, 2018.

Raynaud, D. and Whillans, I.: Air content of the Byrd core and past changes in the West Antarctic ice sheet, Annals of Glaciology, 3, 269–273, https://doi.org/10.3189/S0260305500002901, 1982.

Raynaud, D., Lipenkov, V., Lemieux-Dudon, B., Duval, P., Loutre, M. F., and Lhomme, N.: The local insolation signature of air content in Antarctic ice. A new step toward an absolute dating of ice records, Earth and Planetary Science Letters, 261, 337–349, https://doi.org/10.1016/j.epsl.2007.06.025, https://doi.org/10.1016/j.epsl.2007.06.025, 2007.

Reimer, P. J., Bard, E., Bayliss, A., Beck, J. W., Blackwell, P. G., Ramsey, C. B., Grootes, P. M., Guilderson, T. P., Haflidason, H., and Hajdas, I.: IntCal13 and Marine13 radiocarbon age calibration curves 0–50,000 years cal BP, Radiocarbon, 55, 1869–1887, 2013.

Rhodes, R. H., Faïn, X., Stowasser, C., Blunier, T., Chappellaz, J., McConnell, J. R., Romanini, D., Mitchell, L. E., and Brook, E. J.: Continuous methane measurements from a late Holocene Greenland ice core: Atmospheric and in-situ signals, Earth and Planetary Science Letters, 368, 9–19, https://doi.org/10.1016/j.epsl.2013.02.034, https://doi.org/10.1016/j.epsl.2013.02.034, 2013.

Rhodes, R. H., Brook, E. J., Chiang, J. C., Blunier, T., Maselli, O. J., McConnell, J. R., Romanini, D., and Severinghaus, J. P.: Enhanced tropical methane production in response to iceberg discharge in the North Atlantic, Science, 348, 1016–1019, https://doi.org/10.1126/science.1262005, https://doi.org/10.1126/science.1262005, 2015.

Rhodes, R. H., Brook, E. J., McConnell, J. R., Blunier, T., Sime, L. C., Faïn, X., and Mulvaney, R.: Atmospheric methane variability: Centennial-scale signals in the Last Glacial Period, Global Biogeochemical Cycles, 31, 575–590, https://doi.org/10.1002/2016GB005570, https://doi.org/10.1002/2016GB005570, 2017.

Robin, G. d. Q. and Adie, R. J.: The ice cover, in: Antarctic research: a review of British scientific achievement in Antarctica, edited by Priestley, R. E., Adie, R. J., and Robin, G. d. Q., pp. 100–117, Butterworth & Co Publishers Ltd, London, 1964.

Sapart, C. J., Monteil, G., Prokopiou, M., van de Wal, R. S. W., Kaplan, J. O., Sperlich, P., Krumhardt, K. M., van der Veen, C., Houweling, S., Krol, M. C., Blunier, T., Sowers, T., Martinerie, P., Witrant, E., Dahl-Jensen, D., and Röckmann, T.: Natural and anthropogenic variations in methane sources during the past two millennia, Nature, 490, 85–88, http://dx.doi.org/10.1038/nature11461, 2012.

Schoof, C.: Ice sheet grounding line dynamics: Steady states, stability, and hysteresis, Journal of Geophysical Research: Earth Surface, 112, https://doi.org/10.1029/2006JF000664, 2007.

Schwander, J.: The transformation of snow to ice and the occlusion of gases, in: The Environmental Record in Glaciers and Ice Sheets, edited by Oescher, H. and Langway, C., pp. 53–67, John Wiley, New York, 1989.

Schwander, J., Sowers, T., Barnola, J. M., Blunier, T., Fuchs, A., and Malaize, B.: Age scale of the air in the summit ice: Implication for glacial-interglacial temperature change, Journal of Geophysical Research: Atmospheres, 102, 19 483–19 493, https://doi.org/10.1029/97JD01309, 1997.

Scott, R. F.: The Voyage of the Discovery, vol. 1, Smith, Elder, 1907.

Seltzer, A. M., Buizert, C., Baggenstos, D., Brook, E. J., Ahn, J., Yang, J.-W., and Severinghaus, J. P.: Does $delta^{18}$O of O_2 record meridional shifts in tropical rainfall?, Climate of the Past, 13, 1323–1338, https://doi.org/10.5194/cp-13-1323-2017, https://www.clim-past.net/13/1323/2017/, 2017.

Severinghaus, J. P., Beaudette, R., Headly, M. A., Taylor, K., and Brook, E. J.: Oxygen-18 of O_2 Records the Impact of Abrupt Climate Change on the Terrestrial Biosphere, Science, 324, 1431–1434, https://doi.org/10.1126/science.1169473, https://doi.org/10.1126/science.1169473, 2009.

Shepherd, A., Wingham, D., and Rignot, E.: Warm ocean is eroding West Antarctic ice sheet, Geophysical Research Letters, 31, https://doi.org/10.1029/2004GL021106, 2004.

Shipp, S., Anderson, J., and Domack, E.: Late Pleistocene-Holocene retreat of the West Antarctic Ice Sheet system in the Ross Sea: part 1—geophysical results, Geological Society of America Bulletin, 111, 1486–1516, https://pubs.geoscienceworld.org/gsa/gsabulletin/article-abstract/111/10/1486/183430/late-pleistocene-holocene-retreat-of-the-west?redirectedFrom=fulltext, 1999.

Sigl, M., Fudge, T. J., Winstrup, M., Cole-Dai, J., Ferris, D., McConnell, J. R., Taylor, K. C., Welten, K. C., Woodruff, T. E., Adolphi, F., Bisiaux, M., Brook, E. J., Buizert, C., Caffee, M. W., Dunbar, N. W., Edwards, R., Geng, L., Iverson, N., Koffman, B., Layman, L., Maselli, O. J., McGwire, K., Muscheler, R., Nishiizumi, K., Pasteris, D. R., Rhodes, R. H., and Sowers, T. A.: The WAIS Divide deep ice core WD2014 chronology - Part 2: Annual-layer counting (0-31 ka BP), Climate of the Past, 12, 769–786, https://doi.org/10.5194/cp-12-769-2016, https://doi.org/10.5194/cp-12-769-2016, 2016.

Southon, J., Noronha, A. L., Cheng, H., Edwards, R. L., and Wang, Y.: A high-resolution record of atmospheric ^{14}C based on Hulu Cave speleothem H82, Quaternary Science Reviews, 33, 32–41, 2012.

Sowers, T., Bender, M., and Raynaud, D.: Elemental and isotopic composition of occluded O_2 and N_2 in polar ice, Journal of Geophysical Research: Atmospheres, 94, 5137–5150, https://doi.org/10.1029/JD094iD04p05137, http://dx.doi.org/10.1029/JD094iD04p05137, 1989.

Sowers, T., Bender, M., Labeyrie, L., Martinson, D., Jouzel, J., Raynaud, D., Pichon, J. J., and Korotkevich, Y. S.: A 135,000-year Vostok-Specmap Common temporal framework, Paleoceanography, 8, 737–766, https://doi.org/10.1029/93PA02328, 1993.

Steig, E. J., Fastook, J. L., Zweck, C., Goodwin, I. D., Licht, K. J., White, J. W., and Ackert, R. P.: West Antarctic ice sheet elevation changes, in: The West Antarctic Ice Sheet: Behavior and Environment, edited by Alley, R. B. and Bindschadle, R. A., Antarctic Research Series, pp. 75–90, Wiley Online Library, https://doi.org/10.1029/AR077p0075, 2001.

Stenni, B., Curran, M. A., Abram, N. J., Orsi, A., Goursaud, S., Masson-Delmotte, V., Neukom, R., Goosse, H., Divine, D., Van Ommen, T., et al.: Antarctic climate variability on regional and continental scales over the last 2000 years, Climate of the Past, 13, 1609, https://doi.org/10.5194/cp-13-1609-2017, 2017.

Stone, J. O., Balco, G. A., Sugden, D. E., Caffee, M. W., Sass, L. C., Cowdery, S. G., and Siddoway, C.: Holocene deglaciation of Marie Byrd land, West Antarctica, Science, 299, 99–102, https://doi.org/10.1126/science.1077998, 2003.

Stowasser, C., Buizert, C., Gkinis, V., Chappellaz, J., Schüpbach, S., Bigler, M., Faïn, X., Sperlich, P., Baumgartner, M., Schilt, A., and Blunier, T.: Continuous measurements of methane mixing ratios from ice cores, Atmospheric Measurement Techniques, 5, 999–1013, https://doi.org/10.5194/amt-5-999-2012, http://dx.doi.org/10.5194/amt-5-999-2012, 2012.

Stuiver, M., Denton, G. H., Hughes, T. J., and Fastook, J. L.: History of the marine ice sheet in West Antarctica during the last glaciation: a working hypothesis, in: The Last Great Ice Sheets, edited by Denton, G. H. and Hughes, T. J., pp. 319–436, John Wiley & Sons, New York, 1981.

Svensson, A., Andersen, K. K., Bigler, M., Clausen, H. B., Dahl-Jensen, D., Davies, S., Johnsen, S. J., Muscheler, R., Parrenin, F., Rasmussen, S. O., et al.: A 60,000 year Greenland stratigraphic ice core chronology, Climate of the Past, 4, 47–57, https://doi.org/10.5194/cp-4-47-2008, https://doi.org/10.5194/cp-4-47-2008, 2008.

Thorsteinsson, T. and Waddington, E. D.: Folding in strongly anisotropic layers near ice-sheet centers, Annals of Glaciology, 35, 480–486, https://doi.org/10.3189/172756402781816708, 2002.

Tuohy, A., Bertler, N., Neff, P., Edwards, R., Emanuelsson, D., Beers, T., and Mayewski, P.: Transport and deposition of heavy metals in the Ross Sea Region, Antarctica, Journal of Geophysical Research: Atmospheres, 120, http://dx.doi.org/10.1002/2015JD023293, 2015.

Waddington, E., Conway, H., Steig, E., Alley, R., Brook, E., Taylor, K., and White, J.: Decoding the dipstick: Thickness of Siple Dome, West Antarctica, at the last glacial maximum, Geology, 33, 281–284, https://doi.org/10.1130/G21165.1, 2005.

Waddington, E. D., Bolzan, J. F., and Alley, R. B.: Potential for stratigraphic folding near ice-sheet centers, Journal of Glaciology, 47, 639–648, https://doi.org/10.3189/172756501781831756, 2001.

WAIS Divide Project Members: Onset of deglacial warming in West Antarctica driven by local orbital forcing, Nature, 500, 440–444, https://doi.org/10.1038/nature12376, http://dx.doi.org/10.1038/nature12376, 2013.

Weertman, J.: Stability of the junction of an ice sheet and an ice shelf, Journal of Glaciology, 13, 3–11, https://doi.org/10.3189/S0022143000023327, 1974.

Whitehouse, P. L., Bentley, M. J., and Le Brocq, A. M.: A deglacial model for Antarctica: geological constraints and glaciological modelling as a basis for a new model of Antarctic glacial isostatic adjustment, Quaternary Science Reviews, 32, 1–24, https://doi.org/10.1016/j.quascirev.2011.11.016, 2012.

Winstrup, M.: A Hidden Markov Model Approach to Infer Timescales for High-Resolution Climate Archives, in: AAAI, pp. 4053–4061, 2016.

Winstrup, M., Svensson, A. M., Rasmussen, S. O., Winther, O., Steig, E. J., and Axelrod, A. E.: An automated approach for annual layer counting in ice cores, Climate of the Past, 8, 1881–1895, https://doi.org/10.5194/cp-8-1881-2012, https://doi.org/10.5194/cp-8-1881-2012, 2012.

Winstrup, M., Vallelonga, P., Kjær, H. A., Fudge, T. J., Lee, J. E., Riis, M. H., Edwards, R., Bertler, N. A. N., Blunier, T., Brook, E. J., Buizert, C., Ciobanu, G., Conway, H., Dahl-Jensen, D., Ellis, A., Emanuelsson, B. D., Keller, E. D., Kurbatov, A., Mayewski, P., Neff, P. D., Pyne, R., Simonsen, M. F., Svensson, A., Tuohy, A., and Wheatley, S.: A 2700-year annual timescale and accumulation history for an ice core from Roosevelt Island, West Antarctica, Climate of the Past Discussions, 2017, 1–46, https://doi.org/10.5194/cp-2017-101, https://doi.org/10.5194/cp-2017-101, 2017.

Wolff, E. W., Chappellaz, J., Blunier, T., Rasmussen, S. O., and Svensson, A.: Millennial-scale variability during the last glacial: The ice core record, Quaternary Science Reviews, 29, 2828–2838, https://doi.org/10.1038/ngeo442, 2010.

Figures

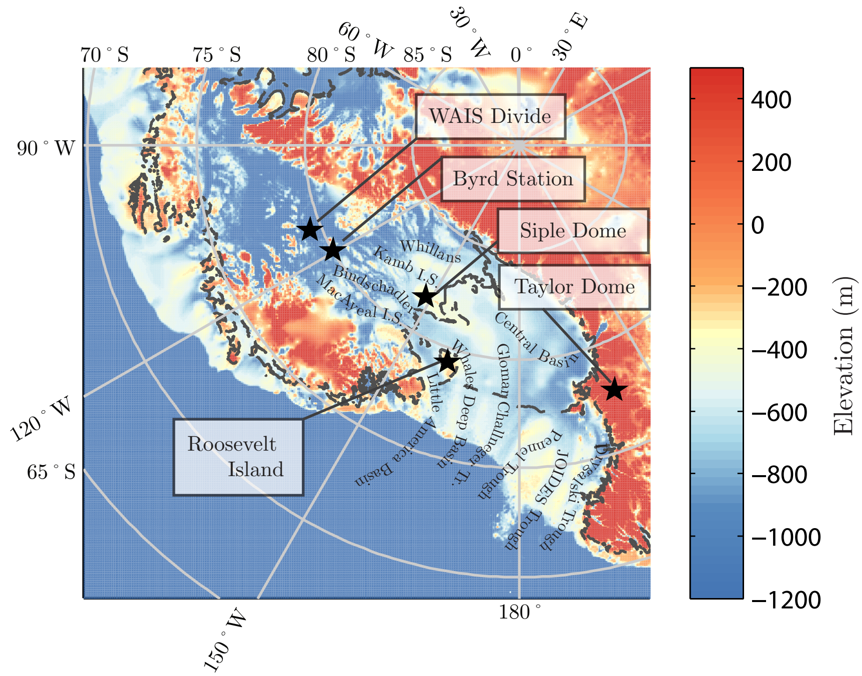

Figure 1. Map of bedrock elevation in the Ross Sea Sector of Antarctica (referenced to WGS84 datum) (Fretwell et al., 2013). Gray dashed lines indicate ice sheet grounding lines and ice margins. Locations of the RICE (Roosevelt Island), Siple Dome, Byrd Station, WAIS Divide, and Taylor Dome ice cores are marked with black stars.

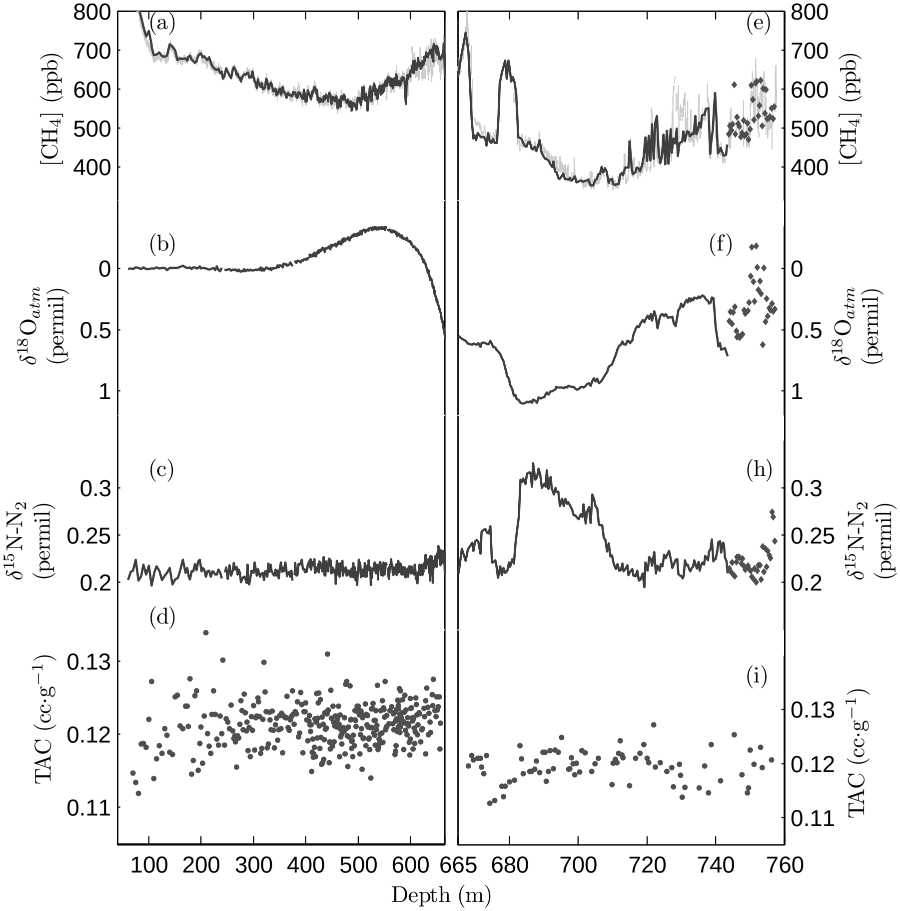

Figure 2. ()Figure was incorrectly labelled and has been updated) Gas data from the RICE ice core. Left panel (a-e) (60-665 m) covers the last 11.26 ka; Right panel (f-j) (665-760 m) covers measurements from 11.26-83 ka and measurements from the 10 m of ice below the dated section. (a, f) Continuous methane measurements, gray, between 0-726 m depth are calibrated to discrete methane measurements, black. Beyond 726 m depth, raw CFA methane measurements are plotted. (b, g) $\delta^{18}O_{atm}$ measurements are corrected for gravitational enrichment in the firn layer using $\delta^{15}N\text{-}N_2$ (c, h) . (d, i) TAC was measured in conjunction with discrete methane.

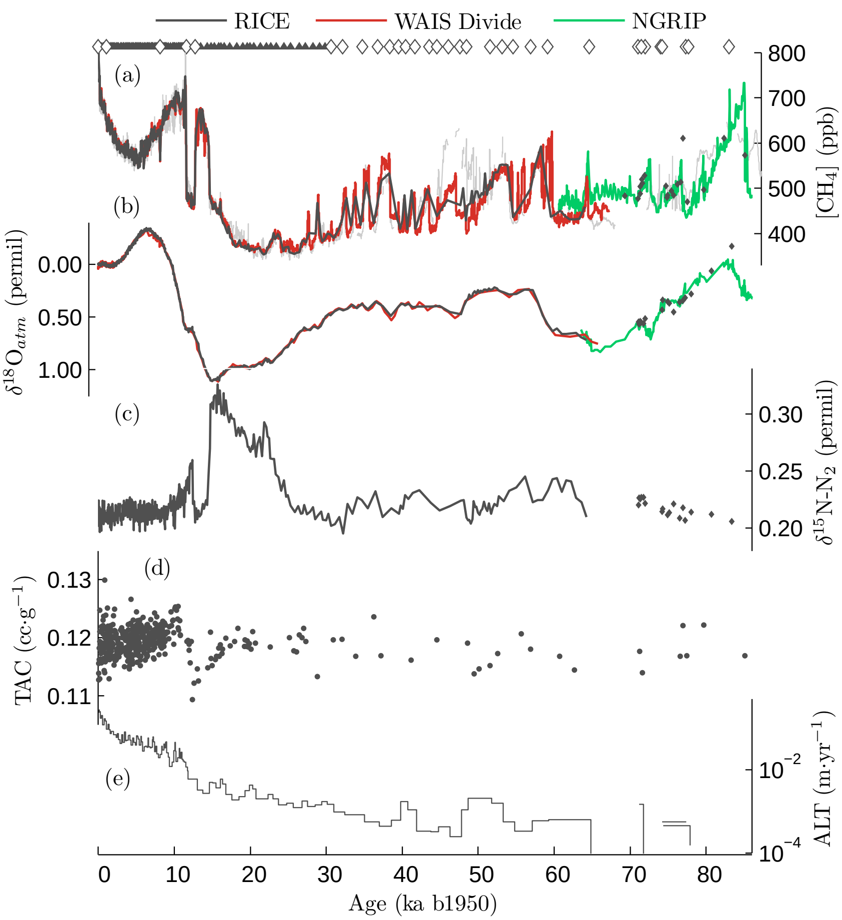

Figure 3. Gas data from the RICE ice core plotted on the RICE17 age scale. (a) RICE methane and (b) $\delta^{18}O_{atm}$ records (gray) shown in comparison to ~~reference~~ target records from the WAIS Divide ice core on the WD2014 age scale (Buizert et al., 2015) (red) and NGRIP ice core (Baumgartner et al., 2014; Landais et al., 2007) on a modified GICC05modelext chronology (Wolff et al., 2010) (green). Solid triangles above panel (a) are gas age constraints from a Monte Carlo analysis, open diamonds are prior ACPs from visual matching. ~~The~~ (c) ~~RICE~~ $\delta^{15}N$-N_2 ~~partially~~ is used to constrain~~s~~ a firn densification model used to estimate the ice age-gas age offset. (d) RICE TAC measurements. (e) Mean annual layer thickness calculated from gas age control points adjusted for Δage.

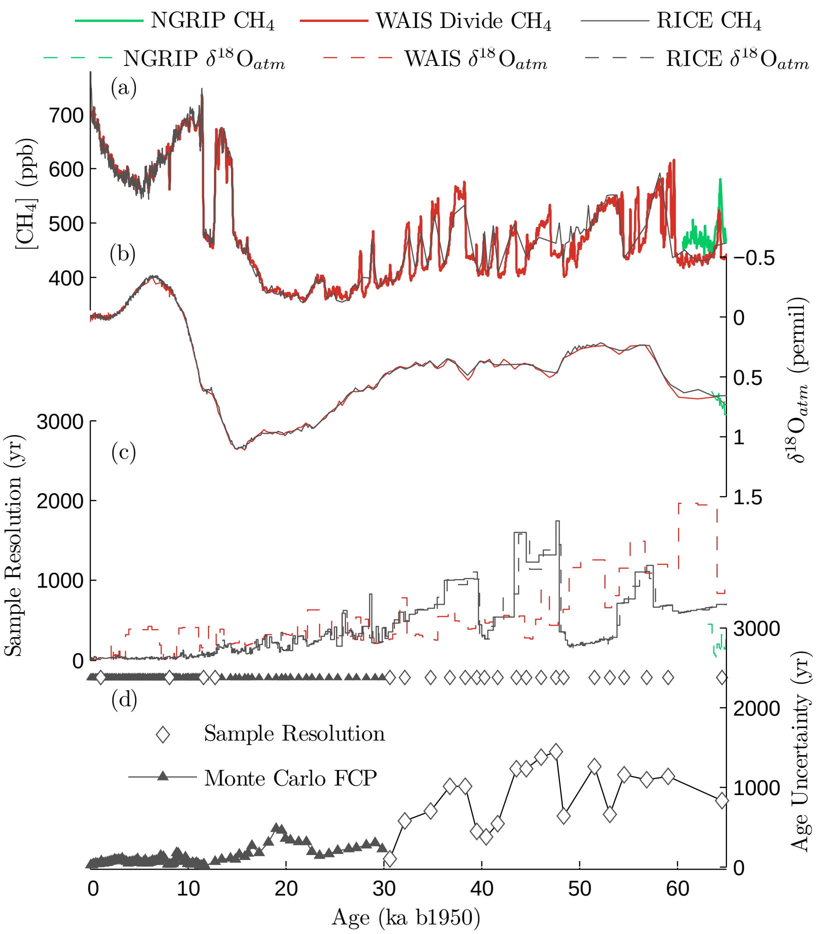

Figure 4. (Figure updated to correct axes label from "sample resolution" to "sample spacing") RICE17 ~~ice core~~ gas age uncertainty. (a) Methane and (b) $\delta^{18}O_{atm}$ records from ~~the~~ RICE (gray), WAIS Divide (Rhodes et al., 2015) (red), and NGRIP ice cores (Baumgartner et al., 2014) (green). (c) Sample ~~resolution~~ spacing for methane (solid lines) and $\delta^{18}O_{atm}$ (dashed lines) for the various cores. (d) Gas age uncertainty, relative to WD2014, for ages determined from a Monte Carlo analysis (solid triangles) and for extended gas age control points (open diamonds).

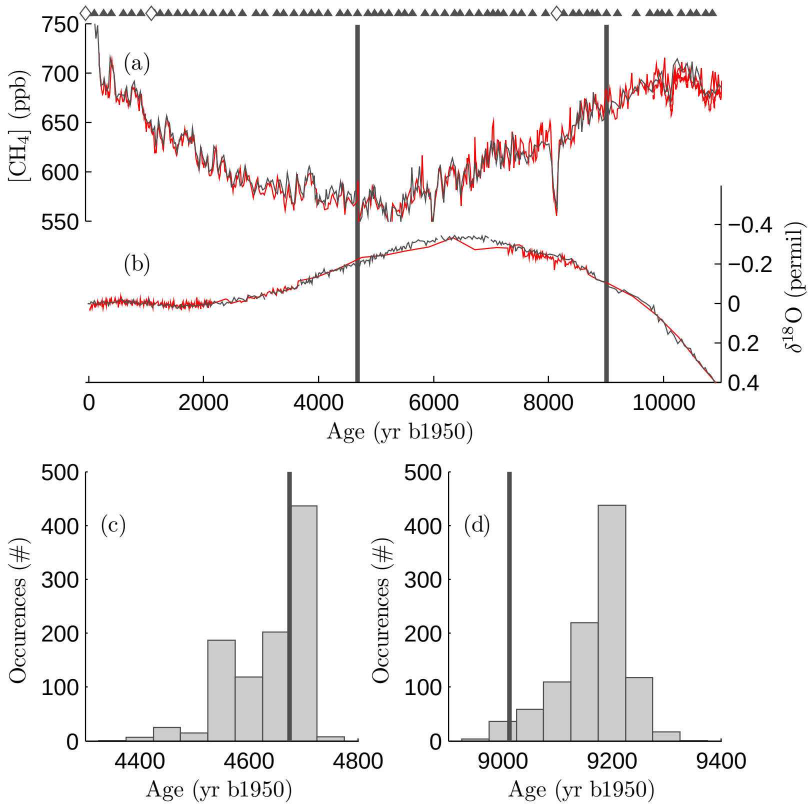

Figure 5. (a) RICE methane and (b) $\delta^{18}O_{atm}$ records matched to those from the WAIS Divide ice core (Rhodes et al., 2015; Buizert et al., 2015) (red lines) ~~between present and~~ for the last 11.7 ka. FCPs from Monte Carlo routine are shown as solid triangles, prior constraints are shown as open diamonds. Lower panels (c, d) show the distribution of the gas ages for two particular depths, 459.05 m (4675 yr BP) (c) and 621.28 m (9012 yr BP) (d) resulting from the Monte Carlo analysis. The final age of these depths, resulting from the best realization, are shown as vertical gray lines.

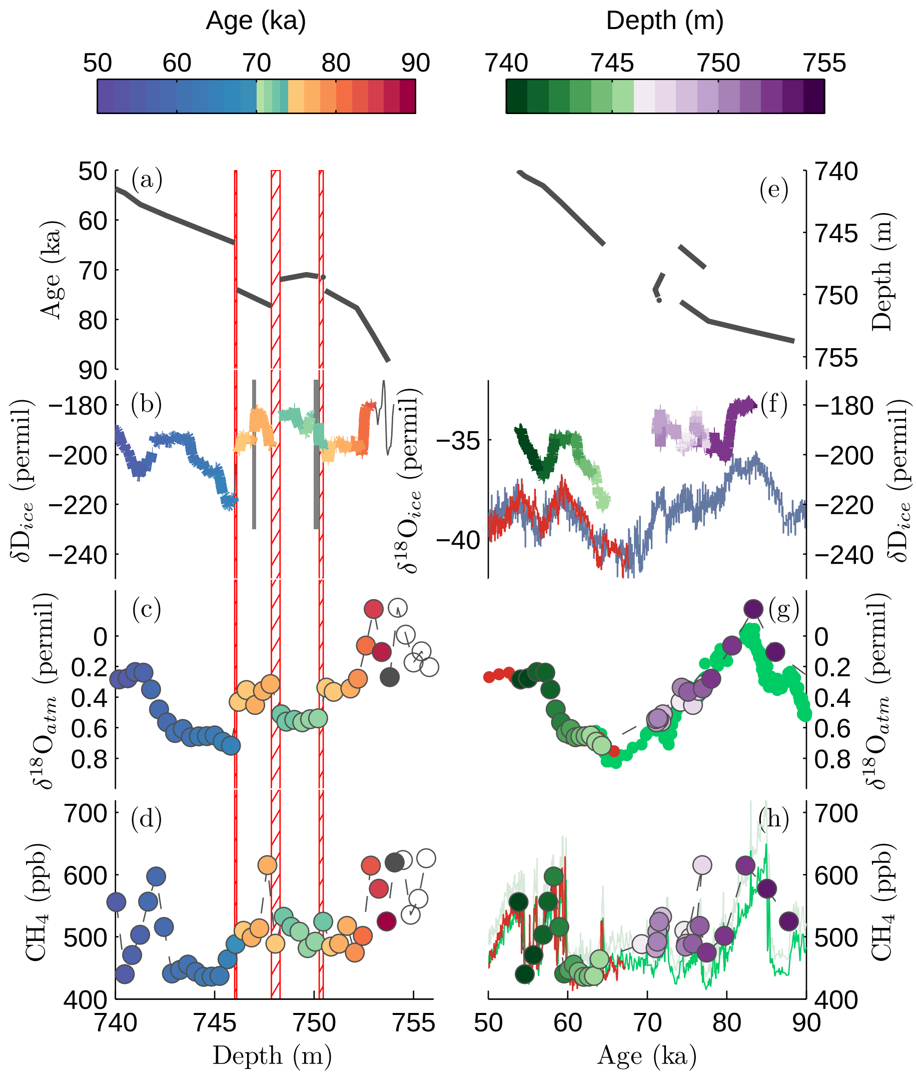

Figure 6. (a) Depth-age relationship from 740-756 m and evidence of an age reversal within the RICE ice core from (b) δD, (c) $\delta^{18}O_{atm}$, and (d) methane data. (b-d) Measurements are plotted against depth and color coded according to the age of the sample. Open circles represent samples for which an age could not be determined. (a-d) Red hatched bars represent discontinuities, where periods of climate history appear to be missing. Solid gray bars in (b) are measurement gaps in the δD record associated with large changes in δD. Repetitions of clusters of data with similar methane and $\delta^{18}O_{atm}$ values best dated to DO-20 are observed both above and below a cluster of depths best dated to DO-19. (e-h) The depth-age relationship and measurements are plotted against the age of the sample and color coded according to depth. WAIS Divide data (red), NGRIP (green), and the EDML $\delta^{18}O_{ice}$ record (blue).

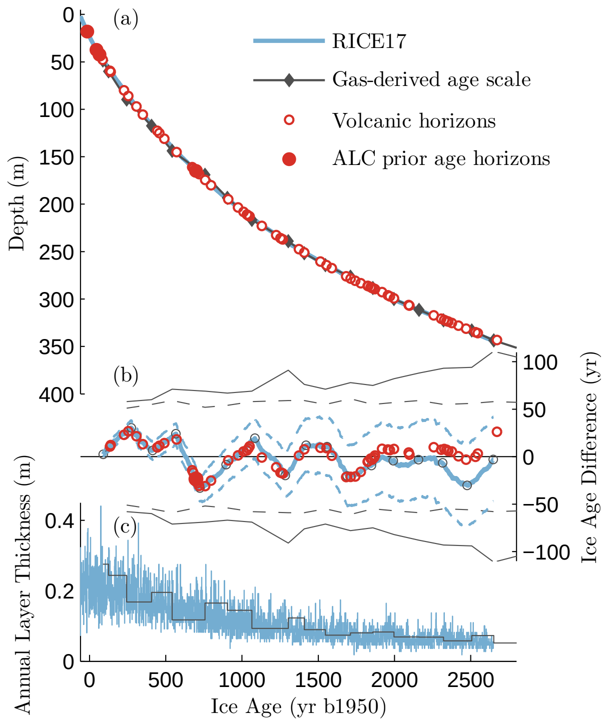

Figure 7. Comparison of the gas-derived (gray) and the annual layer counted ice age-scale (blue, Winstrup et al. 2017). Six absolute age markers (closed red circles) were identified and an additional 67 volcanic horizons were cross correlated to volcanic horizons in the WAIS Divide core (plotted on WD2014 ice age scale, open red circles, Winstrup et al. 2017). (b) Difference in ice age between the gas-derived ice age-scale and annual layer counts; positive values indicate that at the same depth the annual layer counts is older than in the gas-derived age-scale. Uncertainty estimates of the gas-derived ice age-scale (solid gray lines), of the Δage estimate only (dashed gray lines), and of the annual layer counted age scale (blue dashed lines). (c) Interpretations of annual layer thickness from the gas-derived ice age scale and annual layer interpretations.

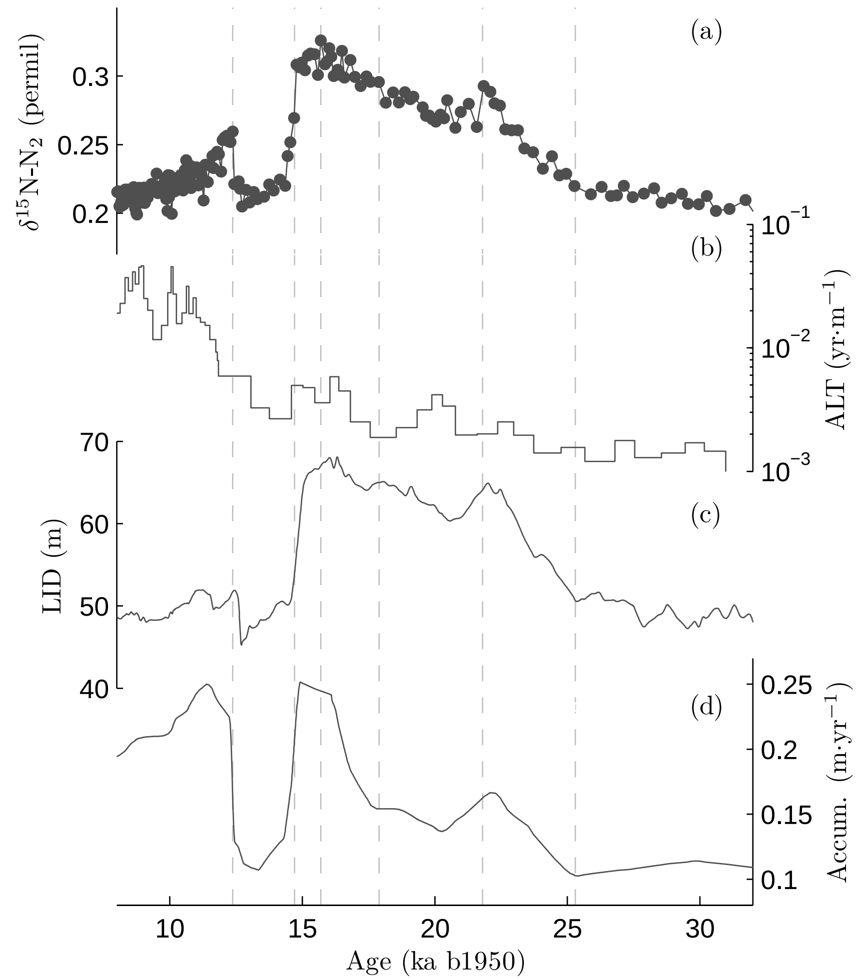

Figure 8. (Updated figure to include CH_4 measurements)Comparison of (a) δ^{15}N-N$_2$, (b) methane concentrations, (c) annual layer thickness implied from depth-age scale, (d) lock-in depth (LID), and (e) accumulation reconstructions from the RICE ice core. Lock-in depth and accumulation is calculated with a dynamic Herron-Langway firn densification model.

Tables

Table 1. Prior gas age constraints and uncertainty are based on matching of features in the atmospheric history of methane and $\delta^{18}O_{atm}$. Name or description of feature are given in the notes and the primary parameter used to identify the feature is provided as the identifying variable. Age uncertainty is related to the duration of the feature.

Depth (m)	Gas_Age (yr)	σ (yr)	Identifying Variable	Notes
48.57	-55.4	7	Modern LID	
239.000	1092	45	CH_4	
591.000	8140	30	CH_4	8.2 ka event
669.150	11580	30	CH_4	Younger-Dryas — Preboreal
677.300	12780	57	CH_4	Bølling-Allerød — Younger Dryas
719.300	30660	100	CH_4	GI 5.1 Termination
720.700	32150		CH_4	GI 5.2 Termination
722.800	34780		CH_4	GI 7 Termination
723.900	36750		CH_4	GI 8 Termination
724.600	38370		CH_4	GI 8 Onset
725.310	39530		CH_4	Mid-GS 9 Methane Event
726.850	40332		CH_4	GI 9 Onset
728.090	41643		CH_4	GI 10 Onset
728.720	43544		CH_4	GI 11 Onset
729.050	44562		CH_4	GI 12 Termination
729.680	46100		$\delta^{18}O_{atm}$	
730.050	47620		$\delta^{18}O_{atm}$	GI 12 Onset
730.950	48420		$\delta^{18}O_{atm}$	Mid-GS 12 Methane Event
737.260	51570		$\delta^{18}O_{atm}$	
739.650	53115		$\delta^{18}O_{atm}$	
740.470	54595		$\delta^{18}O_{atm}$	GI 14 Onset
741.250	56885		$\delta^{18}O_{atm}$	(MIS 4/3 Transition)
742.550	59100		$\delta^{18}O_{atm}$	GI 17.1a Onset (MIS 4/3 Transition)
746.000	64600		δD, $\delta^{18}O_{atm}$, CH_4	Top Depth of discontinuity
746.100	74000		δD, $\delta^{18}O_{atm}$, CH_4	Bottom Depth of discontinuity
747.850	77300		δD, $\delta^{18}O_{atm}$, CH_4	Depth of reversal in δD
748.290	72000		$\delta^{18}O_{atm}$	First $\delta^{18}O_{atm}$ sample clearly in DO-19 grouping
749.600	71000		$\delta^{18}O_{atm}$, CH_4	Depth of youngest part of reversal in δD
750.460	71500		CH_4	Deepest sample clearly related to reversal grouping
750.560	74200		$\delta^{18}O_{atm}$, CH_4	Shallowest sample related to return to DO20 values
752.150	77700		$\delta^{18}O_{atm}$, CH_4	Last $\delta^{18}O_{atm}$ sample clearly part of DO20
752.950	83000		$\delta^{18}O_{atm}$	Minima in $\delta^{18}O_{atm}$, matching values observed in NGRIP and EDML for MIS 5a
753.750	88500		$\delta^{18}O_{atm}$	Enriched $\delta^{18}O_{atm}$, MIS 5b?

Table 2. Model Parameters used for optimized correlation routine. Code for routine can be found in supplementary material.

Variable	Description	0-670 m	670-718.13 m
Model Parameters:			
Runs	# of realizations in Monte Carlo Analysis	1000	1000
N	# of subsections	76	25
Δt	Duration of subsections	154 yrs	726 yrs
k	# of refinements to perturbation	13	13
n_{rep}	# of repetitions before moving to next refinement	20	20
Perturbation Conditions:			
$\overline{A}_{max}$	Maximum "Accumulation"	75 cm·yr^{-1}	75 cm·yr^{-1}
$\overline{A}_{min}$	Minimum "Accumulation"	0 cm·yr^{-1}	0 cm·yr^{-1}
$\Delta t/\Delta t_{prior}$	Relative change in duration of subsection from prior	10x	10x
$\overline{A}_i/\overline{A}_{i-1}$	Maximum relative change of "accumulation rate" between subsequent subsections	2x	2x

Appendix Tables

Table A1. Model Parameters used for steady-state Herron-Langway model.

Description	Mean	σ	Distribution
δ^{15}N-N_2		0.0027‰	normal
Modern temperature	-23.5°C	3°C	normal
Isotope sensitivity	6 ‰·K^{-1}	1.2 ‰·K^{-1}	normal
Surface firn density	400 kg·m^{-3}	.05 kg·m^{-3}	normal
Convective zone thickness	2 m	2 m	uniform
Geothermal induced temperature gradient	-0.6 K	0.6 K	uniform

Table A2. Calibration of the RICE CFA methane dataset is performed by comparison to the RICE discrete methane dataset with corrections for instrument sensitivity and instrument drift. Calibration is done for different segments of the core. Quality of the fit is described by the R^2 statistic comparing calibrated values of the sub-sampled CFA methane record to discrete measurements.

Depth Range	Instr.		Drift	R^2
0-500 m	$C_{final} = C_{raw} \cdot 1.1079 + 25.0900$			0.9854
500-680 m	$C_{final} = C_{raw} \cdot 0.9440 + 10.9337$	+	$t_{meas} \cdot 4.0181 \cdot 10^{-5} - 1.4013 \cdot 10^{-5}$	0.9239
682-726 m	$C_{final} = C_{raw} \cdot 0.8869 + 29.2036$			